Cell Reports
Medicine

Article

SARS-CoV-2 Omicron variant escapes neutralizing antibodies and T cell responses more efficiently than other variants in mild COVID-19 convalescents

Graphical abstract

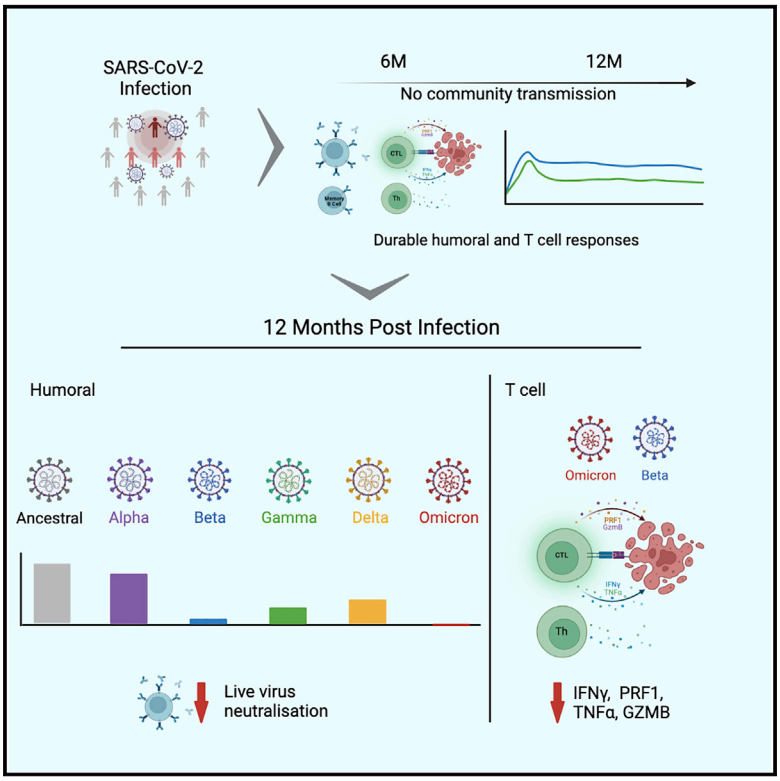

Highlights

- Most mild COVID-19 convalescents maintain immunity at 12 months after disease onset
- B.1.1.529 escapes antibodies in convalescents infected with ancestral SARS-CoV-2
- SARS-CoV-2 VOCs can partially avoid recognition by antigen-specific T cells
- Antigenic drift in SARS-CoV-2 VOCs significantly challenges convalescent immunity

Authors

Pablo Garcia-Valtanen, Christopher M. Hope, Makutiro G. Masavuli, ..., Rowena A. Bull, Simon C. Barry, Branka Grubor-Bauk

Correspondence

simon.barry@adelaide.edu.au (S.C.B.), branka.grubor@adelaide.edu.au (B.G.-B.)

In brief

Garcia-Valtanen et al. investigate immunity in mild COVID-19 convalescents at 12 months after infection in the absence of re-exposure to the virus and vaccination. Both neutralizing antibody and spike-specific T cell responses were significantly affected by the spike amino-acid differences incorporated in B.1.1.529 and other VOCs.

Garcia-Valtanen et al., 2022, Cell Reports Medicine *3*, 100651
June 21, 2022
https://doi.org/10.1016/j.xcrm.2022.100651

CellPress

Cell Reports Medicine

CellPress
OPEN ACCESS

Article

SARS-CoV-2 Omicron variant escapes neutralizing antibodies and T cell responses more efficiently than other variants in mild COVID-19 convalescents

Pablo Garcia-Valtanen,[1,18] Christopher M. Hope,[2,3,18] Makutiro G. Masavuli,[1,18] Arthur Eng Lip Yeow,[1] Harikrishnan Balachandran,[4] Zelalem A. Mekonnen,[1] Zahraa Al-Delfi,[1] Arunasingam Abayasingam,[4] David Agapiou,[4] Alberto Ospina Stella,[5] Anupriya Aggarwal,[5] George Bouras,[6,7] Jason Gummow,[8] Catherine Ferguson,[9] Stephanie O'Connor,[10] Erin M. McCartney,[9] David J. Lynn,[11,12] Guy Maddern,[13] Eric J. Gowans,[1] Benjamin A.J. Reddi,[10] David Shaw,[9] Chuan Kok-Lim,[8,14,15] Michael R. Beard,[15] Daniela Weiskopf,[16] Alessandro Sette,[16,17] Stuart G. Turville,[5] Rowena A. Bull,[4] Simon C. Barry,[2,3,*] and Branka Grubor-Bauk[1,19,*]

[1]Viral Immunology Group, Adelaide Medical School, University of Adelaide and Basil Hetzel Institute for Translational Health Research, Adelaide, SA, Australia
[2]Molecular Immunology, Robinson Research Institute, University of Adelaide, Adelaide, SA, Australia
[3]Women's and Children's Health Network, North Adelaide, SA, Australia
[4]School of Medical Sciences, Faculty of Medicine, UNSW, Australia, Sydney, NSW, Australia
[5]The Kirby Institute, The University of New South Wales, Sydney, NSW, Australia
[6]Adelaide Medical School, Faculty of Health and Medical Sciences, The University of Adelaide, Adelaide, SA, Australia
[7]The Department of Surgery - Otolaryngology, Head and Neck Surgery, University of Adelaide and the Basil Hetzel Institute for Translational Health Research, Central Adelaide Local Health Network, Woodville South, SA, Australia
[8]Gene Silencing and Expression Core Facility, Adelaide Health and Medical Sciences, Robinson Research Institute, University of Adelaide, Adelaide, SA, Australia
[9]Infectious Diseases Department, Royal Adelaide Hospital, Central Adelaide Local Health Network, Adelaide, SA, Australia
[10]Intensive Care Unit, Royal Adelaide Hospital, Central Adelaide Local Health Network and Adelaide Medical School, University of Adelaide, Adelaide, SA, Australia
[11]Precision Medicine Theme, South Australian Health and Medical Research Institute, Adelaide, SA 5001, Australia
[12]Flinders Health and Medical Research Institute, Flinders University, Bedford Park, SA 5042, Australia
[13]Discipline of Surgery, The University of Adelaide, Adelaide, SA 5000, Australia
[14]Microbiology and Infectious Diseases Department, SA Pathology, Adelaide, SA, Australia
[15]Research Centre for Infectious Diseases, School of Biological Sciences, The University of Adelaide, Adelaide, SA, Australia
[16]Center for Infectious Disease and Vaccine Research, La Jolla Institute for Immunology (LJI), La Jolla, CA, USA
[17]Department of Medicine, Division of Infectious Diseases and Global Public Health, University of California, San Diego (UCSD), La Jolla, CA, USA
[18]These authors contributed equally
[19]Lead contact
*Correspondence: simon.barry@adelaide.edu.au (S.C.B.), branka.grubor@adelaide.edu.au (B.G.-B.)
https://doi.org/10.1016/j.xcrm.2022.100651

SUMMARY

Coronavirus disease 2019 (COVID-19) convalescents living in regions with low vaccination rates rely on post-infection immunity for protection against re-infection with severe acute respiratory syndrome coronavirus 2 (SARS-CoV-2). We evaluate humoral and T cell immunity against five variants of concern (VOCs) in mild-COVID-19 convalescents at 12 months after infection with ancestral virus. In this cohort, ancestral, receptor-binding domain (RBD)-specific antibody and circulating memory B cell levels are conserved in most individuals, and yet serum neutralization against live B.1.1.529 (Omicron) is completely abrogated and significantly reduced for other VOCs. Likewise, ancestral SARS-CoV-2-specific memory T cell frequencies are maintained in >50% of convalescents, but the cytokine response in these cells to mutated spike epitopes corresponding to B.1.1.529 and B.1.351 (Beta) VOCs were impaired. These results indicate that increased antigen variability in VOCs impairs humoral and spike-specific T cell immunity post-infection, strongly suggesting that COVID-19 convalescents are vulnerable and at risk of re-infection with VOCs, thus stressing the importance of vaccination programs.

INTRODUCTION

Novel severe acute respiratory syndrome coronavirus 2 (SARS-CoV-2) has infected millions worldwide, causing respiratory coronavirus disease 2019 (COVID-19) and a global pandemic not seen in more than 100 years.[1] Rapid development and deployment of different COVID-19 vaccines and non-pharmaceutical interventions, such as hard and soft lockdowns, are rapidly curbing

numbers of daily new infections, hospitalizations, and deaths in countries where these measures are implemented.[2–7] However, while vaccines represent the most likely way out of the pandemic, antibody responses and neutralizing activity wane over the months following SARS-CoV-2 primary infection[8,9] as well as after immunization with current COVID-19 vaccines.[10,11] SARS-CoV-2 variants with mutations in the spike protein, which enable escape from host antibody responses, add to this problem in convalescents and vaccinees[12–19] and have become a major obstacle to ending this pandemic. So far, five variants, namely, B.1.1.7 (also known as Alpha or UK variant), B.1.351 (Beta, Republic of South Africa [RSA]), P.1 (Gamma, Brazil), B.1.617.2 (Delta, India), and currently B.1.1.529 (Omicron, Botswana and RSA), have stood out for their ability to spread rapidly across different regions of the world (https://covariants.org/), hence earning them the denomination variant of concern (VOC).

After primary infection and in parallel with the antibody response, symptomatic COVID-19 convalescents generate a robust $CD4^+$ and $CD8^+$ memory T cell response that targets a wider range of antigens and epitopes than that covered by antibodies.[20–24] Importantly, the breadth of SARS-CoV-2-specific T cell epitopes appears to be less sensitive to mutations present in VOCs.[25,26] It is unclear to what extent T cells can protect from re-infection and progression to severe COVID-19. However, it is likely that T cell responses in convalescents, which target most SARS-CoV-2 antigens,[20] could afford some level of protection for many months, even years. In fact, SARS-CoV-specific T cells can be detected in convalescents for almost two decades.[27]

While current vaccines are highly effective in preventing severe disease and death, and booster vaccinations may temporarily circumvent dwindling efficacy over time,[28] next-generation vaccines that can prevent virus transmission are likely needed to end the pandemic.[29,30] Long-term studies of the evolution of immune correlates in COVID-19 convalescents, where the immune system has encountered an active live virus infection in the presence of all its antigens, are necessary to elucidate the fine specificities and immune functionality of antibody and T cell responses. In particular, the adaptability of pre-existing immunity to mutated spike antigens, present in VOCs, is the key piece of information that is still unanswered.

Compared with the majority of the world, South Australia is in an optimal position to undertake studies on mid- to long-term immunity of COVID-19 due to (1) early and strict border-control measures with other countries and other states within Australia, which were enforced by health authorities in 2020–2021, thus eliminating local transmission of the virus in the community, and (2) South Australia has maintained a high testing rate with a total test count of >2.2 M with only 899 positive cases, of which only 9 were caused by unknown, locally acquired contacts (accessed on September 23, 2021).[31]

We present a COVID-19 immunity study at 12 months after PCR-confirmed SARS-CoV-2 infection and in the complete absence of community transmission in a South Australian cohort of 43 mild COVID-19 convalescents. An in-depth evaluation of multi-isotype antibody responses, homologous pseudotyped virus, homologous and VOC live-virus serum neutralization activity, receptor-binding domain (RBD)-specific B cell populations, and spike and non-spike SARS-CoV-2-specific $CD8^+$ and $CD4^+$ T cell immunity against ancestral and VOC antigenic epitopes was undertaken. Results were compared with age- and gender-matched COVID-19 naive, healthy individuals and with COVID-19 convalescent responses at 6 months after infection in the same cohort.

RESULTS

Longitudinal SARS-CoV-2 humoral responses in mild-COVID-19 convalescents

The RBD of SARS-CoV-2 spike protein is the main target of neutralizing antibodies (nAbs), and nAb titers decline in the months after COVID-19 infection. In our cohort (Figure 1), although not statistically significant, RBD-specific serum immunoglobulin had a downward trend for all isotypes between the time points analyzed (Figure 1B). The RBD immunoglobulin G (IgG), IgG1, and IgG3 area under the curve (AUC) titers decline was (95% confidence interval [CI]) from 73.0–200.4 to 27.7–81.9, from 66.8–218.2 to 0.8–3.8, and from 0.0-44.3 to 0.18–0.92, respectively (Figure 1B). In comparison with age- and gender-matched (Figure S1) healthy seronegative control AUC values, RBD seropositivity for IgG isotypes was present in the majority of COVID-19 convalescents. This trend was consistent with the presence of above-background levels of circulating memory ($CD27^+$) B cells expressing RBD-specific surface IgG in 88.9% of individuals in the COVID-19 convalescent cohort (95% CI, 153–336 cells/10^6 B cells) compared with healthy controls (95% CI, 0.0–27.9 cells/10^6 B cells) (Figure 1C), indicative of the existence of long-term SARS-CoV-2-specific humoral immunity 12 months post-infection. Spike-specific IgG^+ B cells were also elevated in COVID-19 convalescents, but healthy control background frequencies were also higher (Figure S2), likely due to cross-reactivity. RBD- and spike-specific non-IgG^+ B cell frequencies were present at low rates (Figure S2).

Obtaining long-term serum neutralization data from communities free of circulating SARS-CoV-2, such as in this study, is difficult in other cohorts in the context of this pandemic. In our cohort, sera in 64% of convalescents at 12 months yielded neutralizing titers (ID_{50}) significantly above healthy background levels against the pseudotyped virus bearing a Wuhan-like spike protein, which is the same as the prevalent virus present in the community when study participants were infected (Figure 1D).

Since early 2020, when the study participants were recruited, five VOCs, namely, Alpha (B.1.1.7), Beta (B.1.351), Gamma (P1), Delta (B.1.617.2), and Omicron (B.1.1.529), have dominated the landscape of COVID-19 outbreaks worldwide. Neutralization titers against live-Wuhan virus were 16.8–40.8 (95% CI) with 51.2% of convalescents at 12 months presenting positive neutralizing activity (Figure 1E). Values were similar to those against pseudotyped virus particles bearing the same spike-protein sequence in Figure 1D. As expected, the percentage of patients with positive neutralizing activity against B.1.1.7 virus did not differ significantly (44.2%) to Wuhan, with titers ranging 12.8–29.9 (95% CI). However, a very significant drop in serum neutralization titers was observed for live virus B.1.351 (95% CI, 0.0–2.2), P.1 (0.2–9.9), B.1.617.2 (1.1–10.9), and B.1.1.529 (0.0–0.0) variants, with only 4.6%, 11.6%, 16.2%, and 0% of convalescents, respectively, exhibiting positive neutralization activity (Figure 1E).

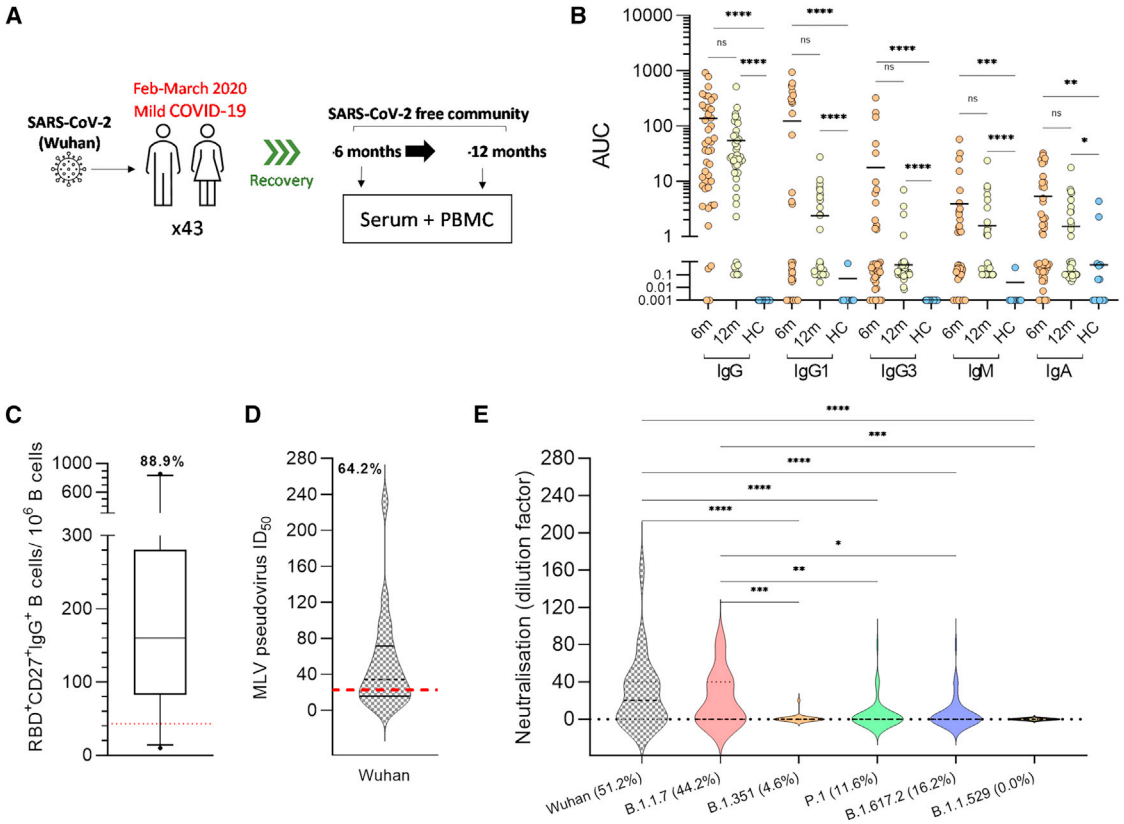

Figure 1. Circulating RBD-specific antibodies, memory B cell frequency, and serum SARS-CoV-2 neutralization activity at 12 months after PCR positive test

(A) Forty-three SARS-CoV-2-infected individuals who presented mild-COVID-19 symptoms were recruited after a PCR positive test, and serum and peripheral blood mononuclear cells (PBMCs) were sampled at 6 and 12 months.

(B) Serum RBD-specific antibody titers, per Ig isotype, reported as area under the curve (AUC) units. Circles represent AUC individual patient values (n = 43 at 6 months, orange, and 12 months, yellow, n = 15 for healthy controls, blue), with mean value denoted by a horizontal black line. Seronegative samples were assigned a value of 0.001 for data visualization purposes.

(C) SARS-CoV-2 RBD-specific (n = 28) memory B cells ($CD27^+$) were quantified 12 months post-infection with corresponding specific tetramers and further characterized as IgG^+. Cell-population-specific background (45.8) was calculated with healthy control PBMCs and shown as a red dashed line.[32] Boxplot shows the 5^{th}–95^{th} percentile range indicating the median value (horizontal line).

(D) Serum neutralization ID_{50} of SARS-CoV-2 and murine leukemia virus (MLV) pseudovirus particles expressing infectious homologous Spike sequence (Wuhan) in mild-COVID-19 convalescent sera (n = 42) at 12 months after positive COVID-19 test. Positive neutralization percentage (indicated above figure) activity cutoff (ID_{50} = 22.61) was calculated from 19 healthy control samples and is shown as a red dashed line.

(E) Patient serum neutralization end-point cut-off titers (highest dilution factor that yields ≥50% inhibition of cell death after live-virus infection) at 12 months against Wuhan, B.1.1.7, B.1.351, P.1, B.1.617.2, and B.1.1.529 live-virus particles. Twenty or 40 was the initial dilution for all serum samples. Neutralization activity was considered negative, value of zero, when neutralization of initial serum dilution was <50%. *p < 0.05, **p < 0.01, ***p < 0.001, and ****p < 0.0001. ns, not significant. The percentage of convalescents with neutralization activity is indicated for each VOC in the corresponding x axis labels.

This is indicative that, despite a high prevalence of RBD seropositivity, the existence of circulating memory B cells, and homologous virus neutralization activity among COVID-19 convalescents, functional humoral responses to VOCs are significantly reduced at 12 months post-infection and are completely abrogated for B.1.1.529 variant.

Longitudinal quantification and phenotyping of SARS-CoV-2 T cell responses in mild-COVID-19 convalescents

Along with antibody responses, the majority of COVID-19 convalescents develop SARS-CoV-2 spike- and non-spike-specific T cell responses.[33] These T cells can be detected and quantified by means of activation-induced marker (AIM) assays using SARS-CoV-2 antigen peptide pools and flow-cytometric analysis (Figure S3).[20,22,23] For accurate interpretation in SARS-CoV-2 AIM assays, naive healthy controls must be included in the analysis to establish assay baseline levels that arise from previous immunity to unrelated antigens/pathogens and particularly to seasonal human coronaviruses.[34] In our cohort, the relative frequency of $CD4^+$ and $CD8^+$ T cells did not differ between the two time points (6 and 12 months) or between COVID-19 convalescents and healthy controls (Figure S4A).

AIM assays revealed that the frequency of circulating spike-specific $CD4^+$ T cells did not significantly decrease between

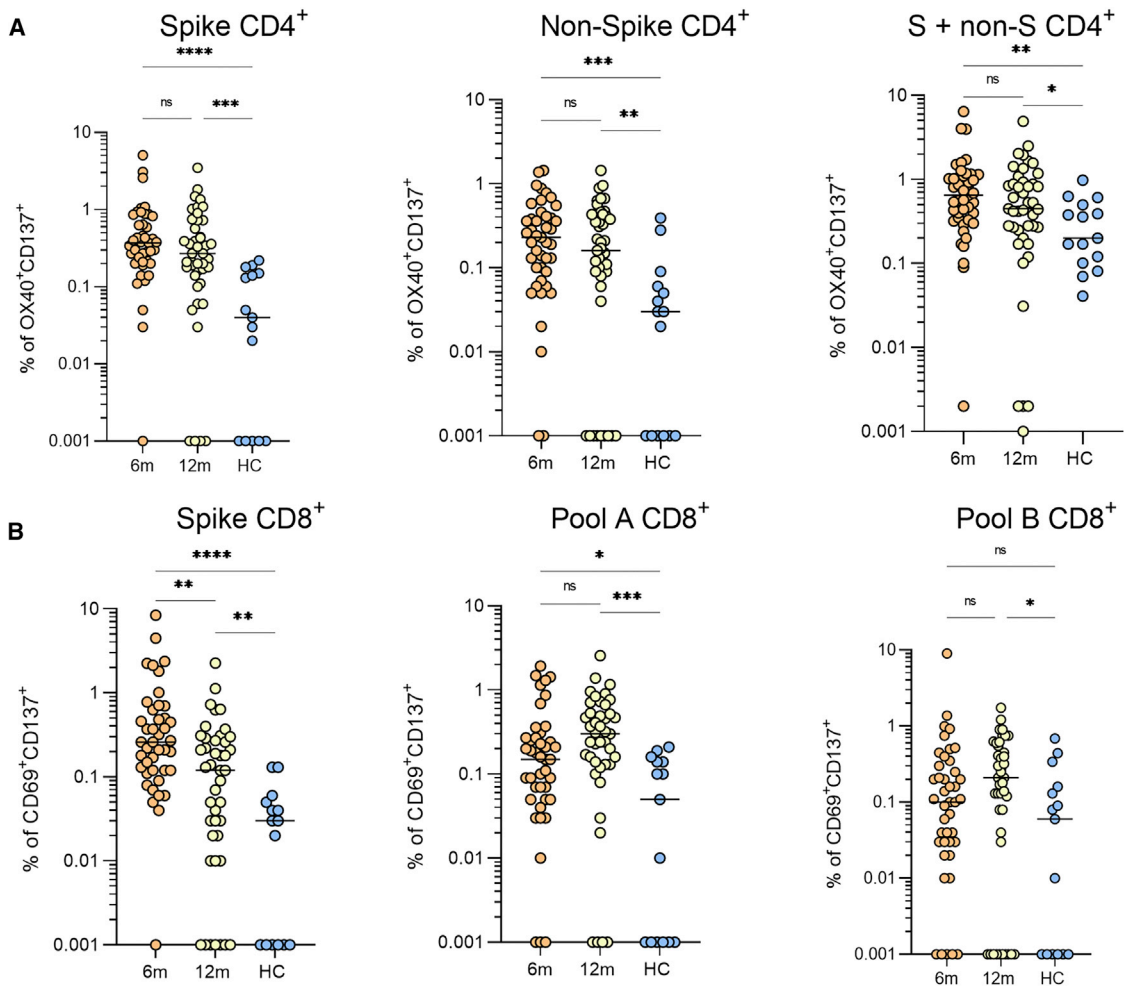

Figure 2. SARS-CoV-2-specific CD4$^+$ and CD8$^+$ T cell frequencies in mild-COVID-19 convalescents at 6 and 12 months after PCR positive test

(A) Percentage of activated CD4$^+$ T cells (OX40$^+$CD137$^+$) after stimulation with spike, non-spike, and cumulative (spike + non-spike) antigen peptide pools within the total CD3$^+$CD4$^+$ T cell population of PBMCs in individual mild-COVID-19 patients (n = 43) at 6 and 12 months after COVID-19 positive test (orange and yellow) and healthy controls (n = 15, in blue).

(B) Percentage of activated CD8$^+$ T cells (CD69$^+$CD137$^+$) after stimulation with spike, whole proteome, and A and B antigen peptide pools within the total CD3$^+$CD8$^+$ T cell population of PBMCs in same samples as in (A).

Dots in (A) represent patient or healthy control individual values. Averages are denoted by a horizontal line, and statistically significant differences between patient and healthy controls are indicated by asterisks. *p < 0.05, **p < 0.01, ***p < 0.001, and ****p < 0.0001. ns, not significant.

6 and 12 months post-infection (95% CI, from 0.35–0.91 at 5–6 months to 0.29–0.68) (Figure 2A). The same trend was observed for non-spike antigen CD4$^+$ T cells (from 0.22–0.43 to 0.18–0.37) and for the combined CD4$^+$ T cell response, spike + non-spike (from 0.60–1.33 to 0.49–1.04) (Figure 2A).

Comparatively, the reduction of spike-specific CD8$^+$ T cell frequency over time was more pronounced and statistically significant (95% CI, from 0.28–1.19 to 0.11–0.35, p < 0.01) (Figure 3B). No statistically significant differences were observed for the frequencies of CD8$^+$ T cells reacting to whole SARS-CoV-2 proteome pools A and B (Figure 2B). Convalescent AIM results were compared with naive healthy controls in all instances, corroborating significantly lower T cell frequencies (baseline levels), consistent with previous AIM studies using the same peptide pools.[22,23] In addition, a positive control consisting of human cytomegalovirus (CMV) protein peptides[22,23,35] was included for all healthy controls and 12 month convalescent data samples. As expected, a high percentage of individuals had a relatively high percentage of CMV-specific T cells (both CD4$^+$ and CD8$^+$) with no significant differences between healthy and convalescent cohorts (Figure S4B). These results are in line with other AIM longitudinal COVID-19 studies spanning from acute phase to up to 10 months after disease onset and indicate sustained maintenance of T cell responses 1 year post-infection.[22,36]

Next, we evaluated the memory phenotype of SARS-CoV-2-specific CD4$^+$ and CD8$^+$ T cells to support stronger conclusions on the specific roles of each population in the maintenance of SARS-CoV-2 immunity. Measuring the expression of surface markers CCR7 and CD45RA allows for the identification of different subsets of memory T cells with different function,

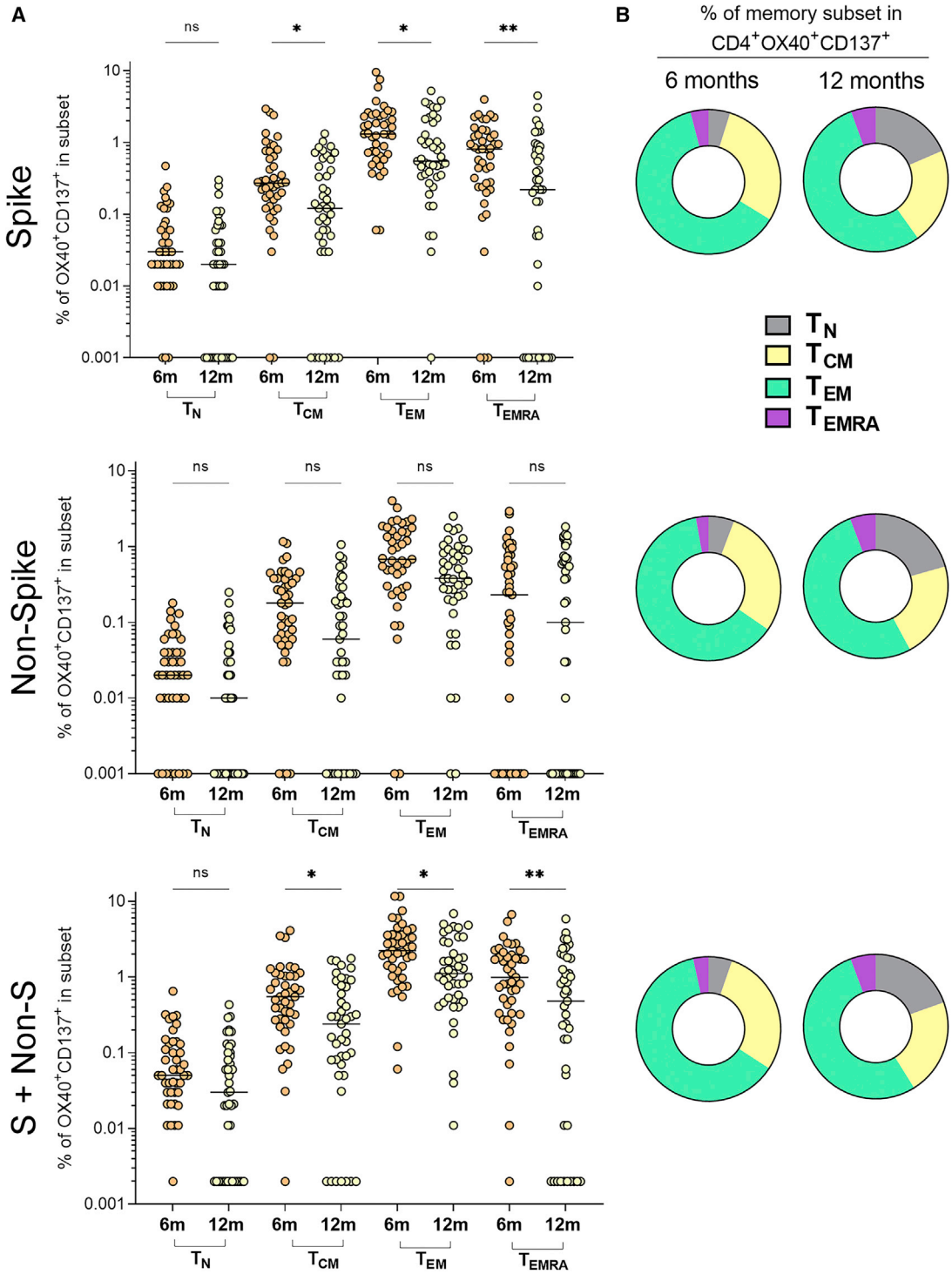

Figure 3. Memory immunophenotyping and quantification of SARS-CoV-2-specific CD4⁺ T cells in mild-COVID-19 convalescents at 6 and 12 months after PCR positive test

(A) Memory immunophenotype based on expression of surface CCR7 and CD45RA of SARS-CoV-2 spike-, non-spike-, and cumulative (spike + non-spike)-specific $CD4^+$ T cells detected in Figure 2A. Cells were classified as follows: naive T cells (T_Ns; $CCR7^+CD45RA^+$), central memory T cells (T_{CM}s; $CCR7^+CD45RA^-$), effector memory T cells (T_{EM}s; $CCR7^-CD45RA^-$), and terminally differentiated effector memory cells re-expressing CD45RA (T_{EMRA}s; $CCR7^-CD45RA^+$).

(legend continued on next page)

kinetics, and frequency depending on the immune status, pathology, and age.[37] In the AIM assay, we assessed the frequencies of SARS-CoV-2-specific T cells within the total pool of central memory T cells (T_{CM}s; $CCR7^+CD45RA^-$), effector memory T cells (T_{EM}s; $CCR7^-CD45RA^-$), terminally differentiated or terminal effector T cells (T_{EMRA}s; $CCR7^-CD45RA^+$), and naive T cells (T_Ns; $CCR7^+CD45RA^+$) in both $CD4^+$ and $CD8^+$ T pools. Between 6 and 12 months post-infection, the frequency of spike-specific $CD4^+$ T cells was significantly reduced in all three memory compartments, T_{CM}s (95% CI, from 0.32–0.73 to 0.17–0.37, $p < 0.05$), T_{EM}s (from 1.2–2.4 to 0.75–1.52, $p < 0.05$), and T_{EMRA}s (from 0.67–1.20 to 0.29–0.85, $p < 0.01$) (Figure 3A). Although the trend is similar for non-spike $CD4^+$ T cell memory subsets, the differences between time points were not statistically significant (Figure 3A). The combined data (spike + non-spike $CD4^+$ T cell subsets) showed statistically significant decrease in SARS-CoV-2-specific $CD4^+$ T_{CM}s (from 0.51–1.06 to 0.28–0.60, $p < 0.05$), T_{EM}s (from 2.11–3.68 to 1.22–2.24, $p < 0.05$), and T_{EMRA}s (from 0.98–1.83 to 0.58–1.37, $p < 0.01$) (Figure 3A). Importantly, the T_{EM} phenotype was clearly predominant in SARS-CoV-2-specific $CD4^+$ T cells, making up >60% and >50% of all $CD4^+OX40^+CD137^+$ at 6 and 12 months, respectively, irrespective of antigen specificity (Figure 3B).

Analysis of the SARS-CoV-2-specific memory $CD8^+$ T cells revealed important differences compared with $CD4^+$ T cells. Predominant $CD8^+$ T_{EMRA}s specific to SARS-CoV-2 suffered a pronounced reduction regardless of antigen specificity. The frequency of spike-specific $CD8^+$ T_{EMRA}s decreased from 0.66–1.96 to 0.23–0.70 (95% CI, $p < 0.001$) as well as for the for SARS-CoV-2 whole proteome (from 0.38–0.92 to 0.07–0.38, $p < 0.001$, for pool A and from 0.12–1.18, to 0.02–0.34, $p < 0.001$, for pool B) (Figure 4A). The importance of T_{EMRA}s within the $CD8^+$ T pool in COVID-19 convalescents was further highlighted, as they were the predominant cell subset within $CD8^+CD69^+CD137^+$cells at 6 (>65%) and at 12 months (>60%), irrespective of antigen specificity (Figure 4B).

The presence of significant frequencies of SARS-CoV-2 antigen-specific $CD4^+$ T_{EM}s and $CD8^+$ T_{EMRA}s at 12 months has important implications, particularly in the absence of virus re-exposure, given that, in principle, these cells have a limited lifespan. Importantly, a significant decrease in these populations from 6 to 12 months suggests that in the absence of re-stimulation by either infection or vaccination, these populations will eventually not be detectable in circulation or will plateau at low frequencies for extended periods of time. In the future, the nature of the renewal mechanisms of both of these cell populations is an important question that needs to be addressed.

Functionality of spike-specific T cells in "high-responder" convalescents

A direct indicator of T cell effector function is their ability to produce immunomodulatory cytokines upon antigen stimulation. Because spike was the immunodominant SARS-CoV-2 antigen according to our AIM results (Figure 2), we selected COVID-19 convalescents with spike-specific $CD4^+$ and $CD8^+$ T cell responses well above healthy control levels (mean plus 3× standard deviations) (Figure 5A), hereafter referred to as high responders. We performed a spike-specific $CD4^+$ and $CD8^+$ T cell intracellular cytokine staining (ICS) assay measuring the pleiotropic signaling cytokines interferon gamma (IFNγ) and tumor necrosis factor alpha (TNF-α) as well as the cytotoxic enzymes granzyme B (GZMB) and perforin (PRF1) and T cell-activation factor interleukin-2 (IL-2). Additionally, we evaluated the frequency and functionality of spike-specific circulating T follicular helper cells (cT_{FH}s) given their importance for immune memory in COVID-19 convalescents[22,38] (see Figures S5 and S6 for ICS/cT_{FH} gating strategy).

At 12 months post-infection, the frequency (%) of spike-specific cT_{FH} cells in COVID-19 convalescents was not significantly different (95% CI, 0.21%–1.48%) from that of healthy controls (0.05%–0.27%) (Figure 5B). The frequency of $IFN\gamma^+$ (Figure 5B), TNFα-, GZMB-, PRF1-, or IL-2- (Figure S7) positive cT_{FH} cells also did not differ from that of healthy controls.

The reactivity of $CD4^+$ T cells in high-responder convalescents to the whole spike protein was dominated by a higher percentage of $CD4^+$ T cells expressing IFNγ (95% CI, 0.02%–0.26%, $p < 0.001$) and TNF-α (0.02%–0.16%, $p < 0.01$) (Figure 5C). The percentages of $CD4^+$ T cells expressing GZMB, PRF1, and IL-2 were not significantly higher than in healthy controls (Figure 5C). In agreement with their known cytotoxic function, spike-specific $CD8^+$ T cells in COVID-19 convalescents exhibited high frequencies of GZMB (95% CI, 1.43%–12.30%, $p < 0.01$) and PRF1 (2.56%–11.27%, $p < 0.001$), while IFNγ-, TNFα-, or IL-2-expressing cells were not significantly different (Figure 5D). Taken together, our AIM and ICS data clearly show a durable, multifunctional response of circulating helper and cytotoxic T cells 12 months post-COVID-19. Importantly, we show that cT_{FH} frequencies and their effector function were diminished.

T cell specificity to VOC spike-mutated sequences in mild-COVID-19 high responders

Recent studies suggest that T cell specificity to whole spike antigen and other SARS-CoV-2 proteins is relatively unaffected by the changes in spike amino-acid sequences characteristic of current VOCs.[25] However, these studies have either used peptide pools covering both mutated and non-mutated regions of individual antigens (spike and non-spike),[25] in which mutated peptides represent a very small proportion of the overall pool. Hence, any differences in T cell specificities and functionality against the mutations in the spike antigen of VOCs were potentially masked. Importantly, while it is possible that overall SARS-CoV-2 T cell epitope recognition is largely unaffected by antigen VOC mutations, it has been postulated that changes in single or

Frequencies are indicated as the percentage of total SARS-CoV-2 antigen-specific $CD4^+$ T cells within the total pool of immune cells with same phenotype in the patient's PBMCs.
(B) Doughnut charts indicating the proportion (%) of each immune phenotype in (A) of the total of SARS-CoV-2-specific $CD4^+$ T cells for each antigen.
In (A), circles represent patient individual values. Averages are denoted by a horizontal line, and statistically significant differences between time points are indicated by asterisks. *$p < 0.05$ and **$p < 0.01$. ns, not significant.

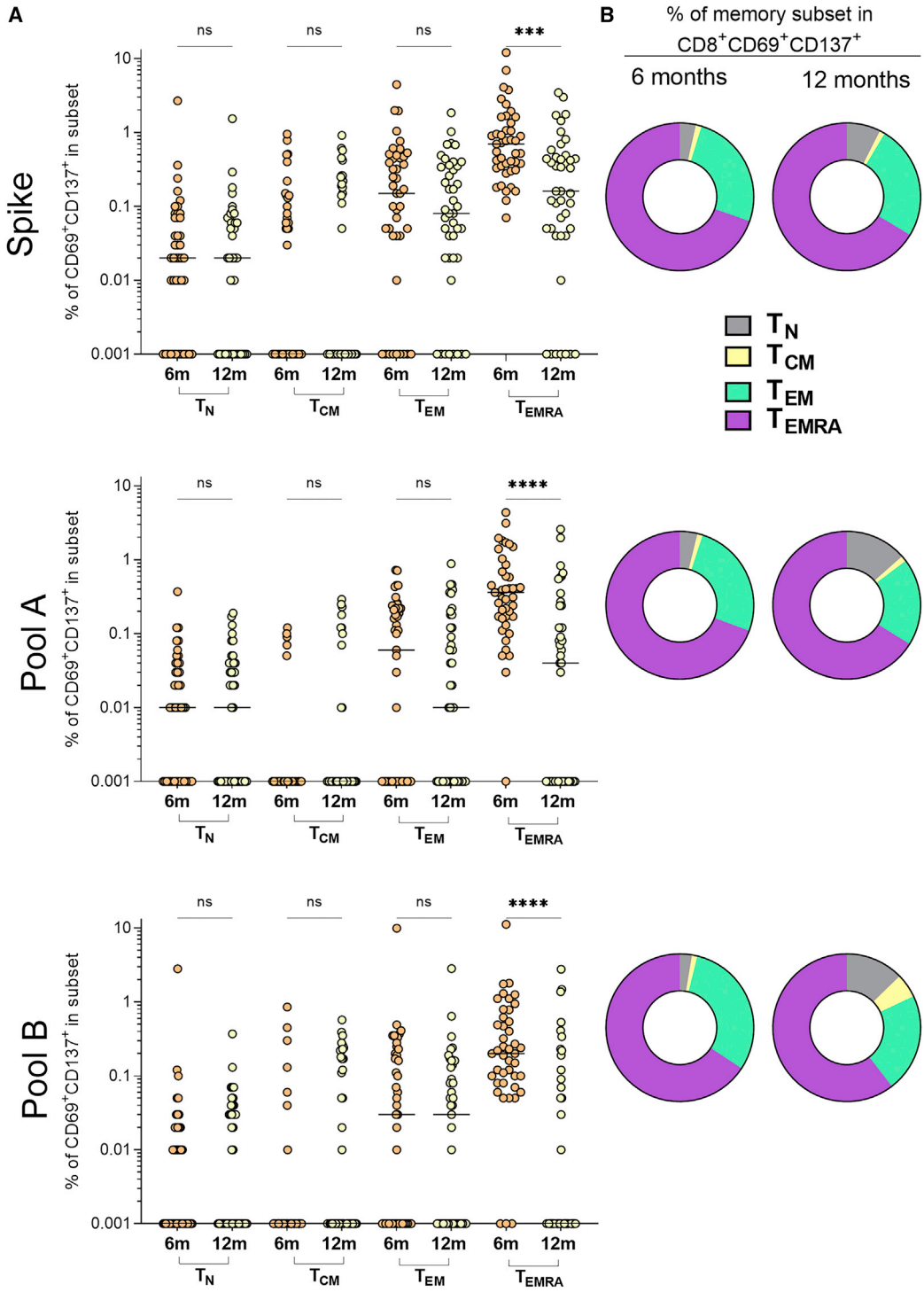

Figure 4. Memory immunophenotyping and quantification of SARS-CoV-2-specific CD8$^+$ T cells in mild-COVID-19 convalescents at 6 and 12 months after PCR positive test

(A) Memory immunophenotype based on expression of surface CCR7 and CD45RA of SARS-CoV-2 spike- and whole proteome pools A- and B-specific CD8$^+$ T cells detected in Figure 2B. Immune phenotypes were defined as in Figure 3. Frequencies are indicated as the percentage of total SARS-CoV-2 antigen-specific CD8$^+$ T cells within the total pool of immune cells with same phenotype in the patient's PBMCs.

(B) Doughnut charts indicating the proportion (%) of each immune phenotype in (A) of the total of SARS-CoV-2-specific CD8$^+$ T cells for each antigen. In (A), circles represent patient individual values. Averages are denoted by a horizontal line, and statistically significant differences between time points are indicated by asterisks. ***$p < 0.05$ and ****$p < 0.01$. ns, not significant.

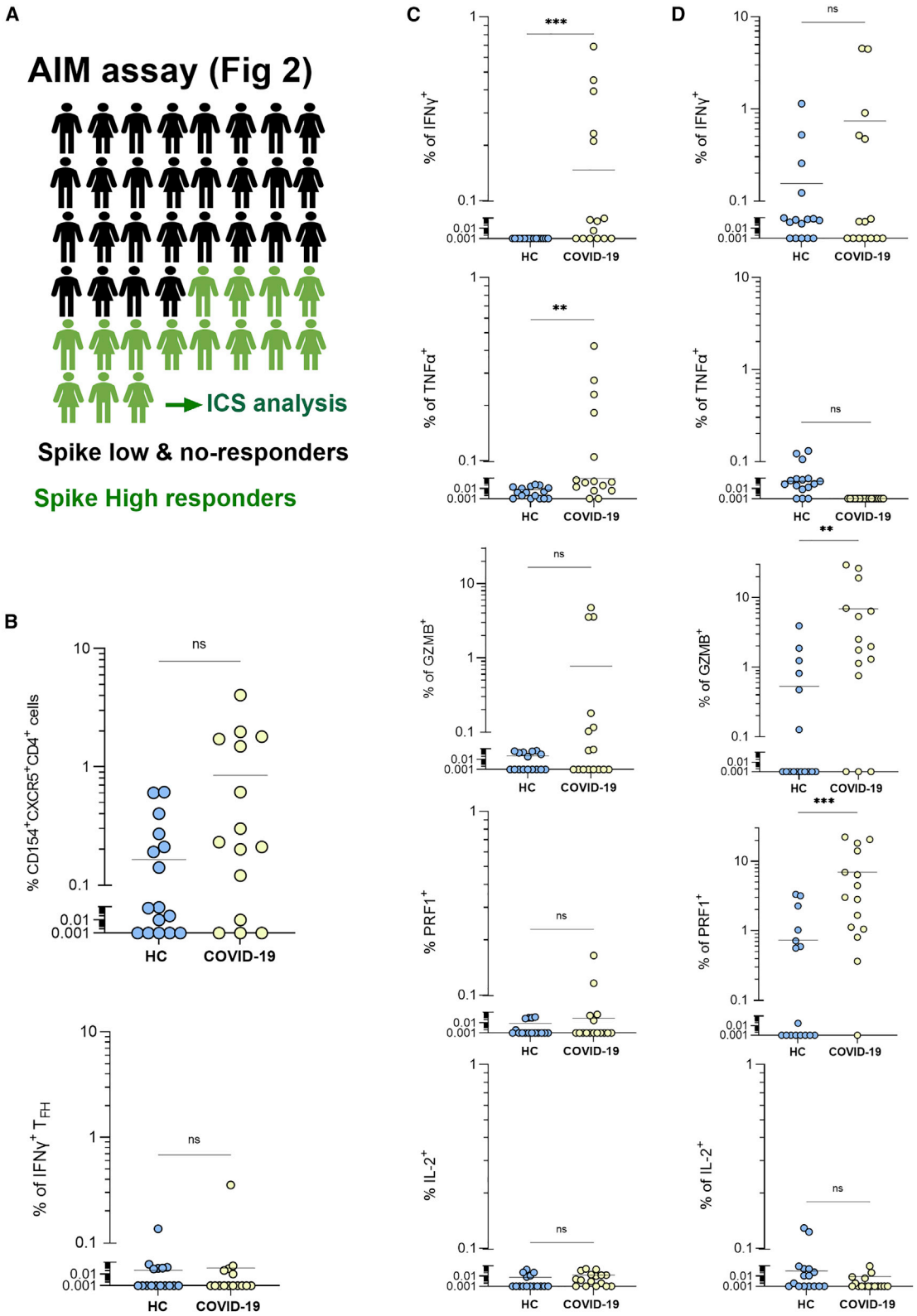

(legend on next page)

few immunodominant epitopes could contribute to VOC escape from T cell response and variant selection.[39] Others before us used mutation-specific spike peptides but only for B.1.1.7 and B.1.351 VOCs.[26] Here, we have tested T cell specificity and functionality to the spike proteins of all five VOCs with peptide pools covering corresponding mutated regions by ICS in high-responder COVID-19 convalescents (n = 15) matching reagents and analysis strategies (Figures S8 and S9) from previous studies to allow for relevant comparisons.[25,26]

For the context of this experiment and its results, it is important to note that our cohort was infected in early 2020 in Australia, where SARS-CoV-2 with unmutated spike amino-acid sequences was prevalent (Figure 6A). In order to clearly identify changes in functionality of T cell immunity to spike antigens present in VOCs, we calculated the fold change of cytokine-positive-expressing cells relative to cells from the same convalescents stimulated with equivalent peptide pools bearing amino-acid sequences corresponding to ancestral (Wuhan) SARS-CoV-2 spike protein (Figure S10). Overall, the data show that $CD4^+$ T cell cytokine expression (Figure 6B) was more affected by VOC mutations than corresponding cytokine responses in $CD8^+$ T cells (Figure 6C). Cytokine-expressing cell fold-change values indicated that mutations present in B.1.1.529 spike resulted in significantly lower expression of IFNγ (95% CI, -1.86 to 1.42), TNF-α (-5.90 to -0.19), and GZMB (-3.85 to 1.52) by $CD4^+$ T cells and IFNγ (-12.46 to -0.30) and IL-2 (-4.78 to 1.42) by $CD8^+$ T cells when compared with other VOCs (Figures 6B and 6C). This difference was most obvious for $CD4^+$ T cell TNF-α, where statistically significant differences were found between B.1.1529 and all other VOCs (Figure 6B). A notable decrease in GZMB expression by $CD4^+$ T cells in response to B.1.351 spike-mutated epitopes was observed (95% CI, -8.24 to 0.24; $p < 0.01$ with B.1.1.7 and P.1, $p < 0.05$ with B.1.1.529). Similarly, B.1.351 spike epitope-induced cytokine expression was reduced for IFNγ and PRF1 in $CD4^+$ T cells compared with P.1 and B.1.617.2 ($p < 0.05$, Figure 6B) and for IFNγ in $CD8^+$ T cells compared with B.1.617.2 ($p < 0.001$; Figure 6C). Notably, GZMB and PRF1 expression in $CD8^+$ T cells was completely unaffected by changes in the spike sequence (Figure 6C), suggesting that cellular cytotoxic immune function may be most resistant to antigenic changes.

To further analyze our data, we used a cut-off fold-change value of -2, meaning a 2-fold reduction in the frequency of cytokine-expressing cells to mutated VOC spike peptides (compared with homologous Wuhan peptides), and observed that individual convalescent responses to spike VOCs were widely heterogeneous, with four convalescents out of 15 accumulating 47% of all 2-fold downregulated values (Figure S11A). With the same criterion, reductions in cytokine-expressing cells occurred more in $CD4^+$ T cells (83 out of 114) than in $CD8^+$ T cells (31 out of 114) (Figure S11B). IFNγ and TNF-α were similarly affected by VOC mutations in $CD4^+$ T cells (25% and 27% of all 2-fold reductions) while in $CD8^+$ T cells, IFNγ was most influenced by VOC spike mutations, with 52% of all 2-fold reductions (Figure S11B). In terms of which VOC evades T cell cytokine responses more efficiently, over one-third of all 2-fold reductions was measured in cells stimulated with mutated peptides corresponding to B.1.1.529 (35.1% of the total), followed by B.1.351 (23.7%), B.1.17 (16.7%), B.1.617.2 (15.8%), and P.1 (8.8%) (Figure S11C).

Here, we report that a loss of spike-specific T cell functionality against VOCs, despite durable (12 months) maintenance in overall frequency, in COVID-19 convalescents. These data suggest that suboptimal spike-specific T helper cell functional responses are more likely to occur in convalescents (infected with Wuhan-like variants) who encounter B.1.351 or B.1.1.529 rather than other VOCs. Our data show that spike-specific T cell IFNγ and TNF-α responses are more likely to be affected. This is similar to what happens with humoral antibody responses in COVID-19 convalescents and vaccinees[12,16,18] and is further supported by our live-virus neutralization data (Figure 1E).

Immune-parameter correlations

When the immune-correlate data were analyzed as a whole (Figure 7), we observed a degree of correlation between RBD-IgG levels and live-virus neutralization (Figure 7A, top left quadrant) except for the B.1.1.529 variant, where neutralization was completely absent. The pattern of correlation between cellular immunity metrics was highly dependent on time (6 or 12 months after COVID-19) and the major T cell phenotype, that is, $CD4^+$ or $CD8^+$ (Figures 7A and 7B). Interestingly, the levels of RBD-IgG3 (Figure 7A, first row) were negatively correlated with frequencies of spike- and non-spike antigen $CD4^+$ and $CD8^+$ T cells. The frequencies of non-Spike $CD4^+$ T_{EM}s at 12 months after COVID-19 positively correlated with total antigen (spike + non-spike) frequencies of multiple $CD4^+$ T cell memory subtypes at 6 months post-COVID-19 (Figure 7A). Finally, in the high-responder cohort, cytokine data revealed that the frequency of spike-specific $CD4^+$ T cells expressing TNF-α and IFNγ and $CD8^+$ T cells expressing PFR1, GZMB, and IFNγ positively correlated (Figure 7C).

Figure 5. Cytokine expression and circulating T follicular helper cell frequencies in convalescents with strong T cell immune responses to SARS-CoV-2 spike protein

(A) Fifteen Spike high-responder convalescents exhibiting high spike-specific $CD4^+$ and $CD8^+$ T cell frequencies in the AIM assay (Figure 2) were further analyzed for spike-specific cT_{FH} and intracellular cytokine staining (ICS) analysis using the whole spike peptide pool.

(B) Frequency of circulating spike-specific T follicular helper cells ($CD4^+CXCR5^+iCD154^+$) in healthy controls (n = 15) and selected high-responder convalescents (n = 15) and percentage of $IFN\gamma^+$ cells.

(C) Percentage of cytokine-positive expression in $CD3^+CD4^+iCD154^+$ T cells in the same individuals as (B).

(D) Percentage of cytokine-positive expression in $CD3^+CD8^+$ T cells in the same individuals as (B).

In (B)–(D), circles represent healthy or patient individual values. Averages are denoted by a horizontal line, and statistically significant differences between time points are indicated by asterisks. **$p < 0.01$ and ***$p < 0.001$. ns, not significant.

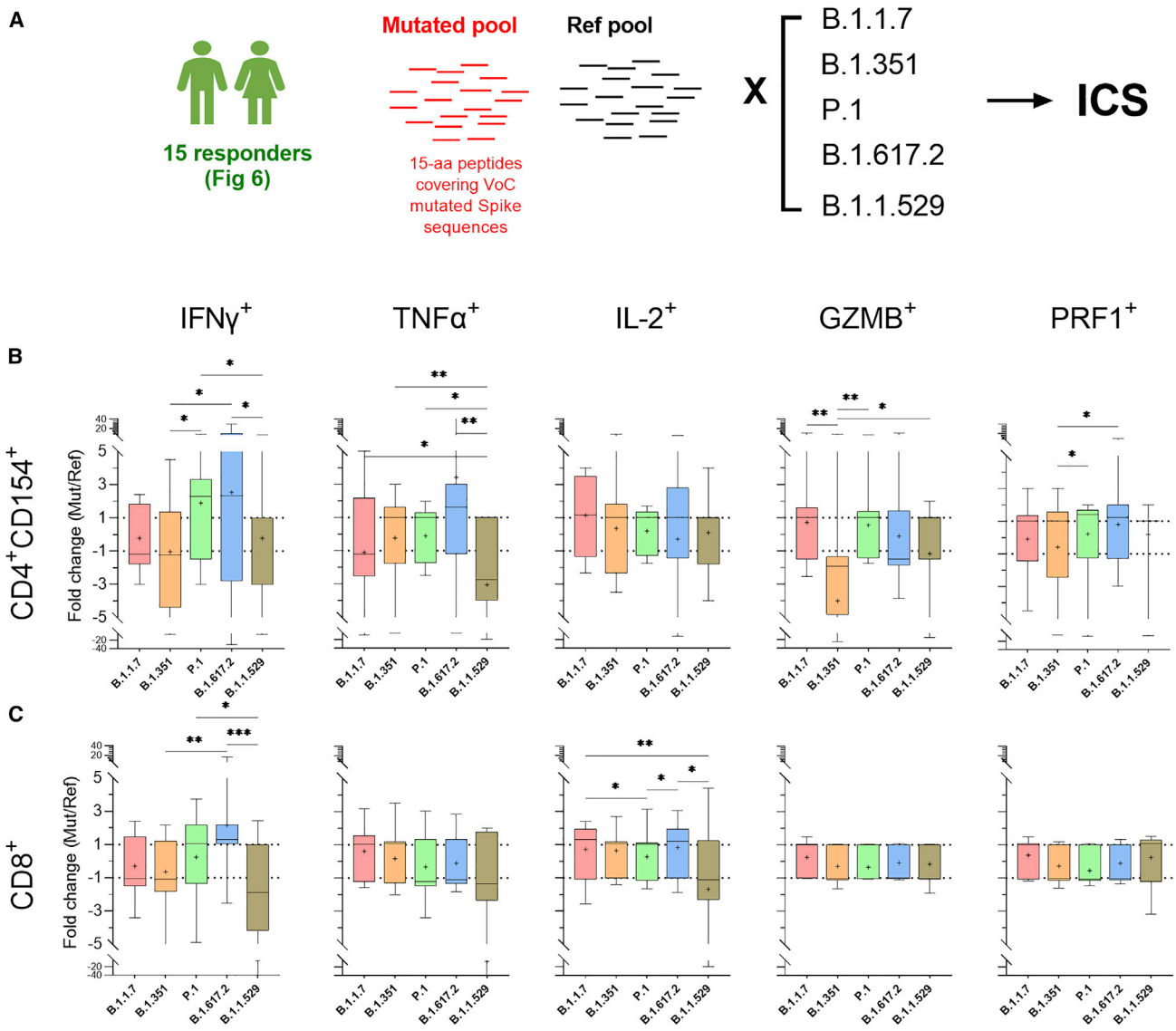

Figure 6. Specific T cell responses in responder convalescents to mutated spike amino-acid sequences in VOCs

(A) PBMCs from spike high responders (n = 15, same as in Figure 5) were stimulated with peptides covering mutated spike regions in VOCs, and cytokine expression was measured by ICS.

(B) Fold-change cytokine expression in $CD3^+CD4^+iCD154^+$ T cells. Negative folds denote decrease in cytokine expression when stimulated with mutated peptide pools. Dotted lines indicate folds (-1 and 1, no change). Boxplots represent interquartile-range values, and whiskers represent minimum and maximum values. Horizontal lines and crosses inside boxplots denote median and mean values, respectively.

(C) Fold-change cytokine expression in $CD3^+CD8^+$ T cells. Negative folds denote decrease in cytokine expression when stimulated with mutated peptide pools. Dotted lines indicate folds (−1 and 1, no change). Boxplots represent interquartile-range values, and whiskers represent minimum and maximum values. Horizontal lines and crosses inside boxplots denote median and mean values, respectively.

(Statistically significant differences between variants for each cytokine and cell type are indicated by asterisks. *$p < 0.05$, **$p < 0.01$, and ***$p < 0.001$.

DISCUSSION

The evidence from large observational studies in healthcare workers and the general population suggests that SARS-CoV-2 immunity post-infection confers a level of protection against COVID-19.[40–42] One caveat of these studies is that high rates of transmission of SARS-CoV-2 in the communities where the studies were conducted (e.g., Italy, UK, or the United States) increased the likelihood of virus re-exposure in these cohorts, precluding the ability to draw firm conclusions on the duration and protective effects of primary SARS-CoV-2 immunity.

Controlled, in-depth studies in convalescents have also been conducted, but vaccination and almost ubiquitous high SARS-CoV-2 infection rates have reduced the opportunities to recruit

CellPress
OPEN ACCESS

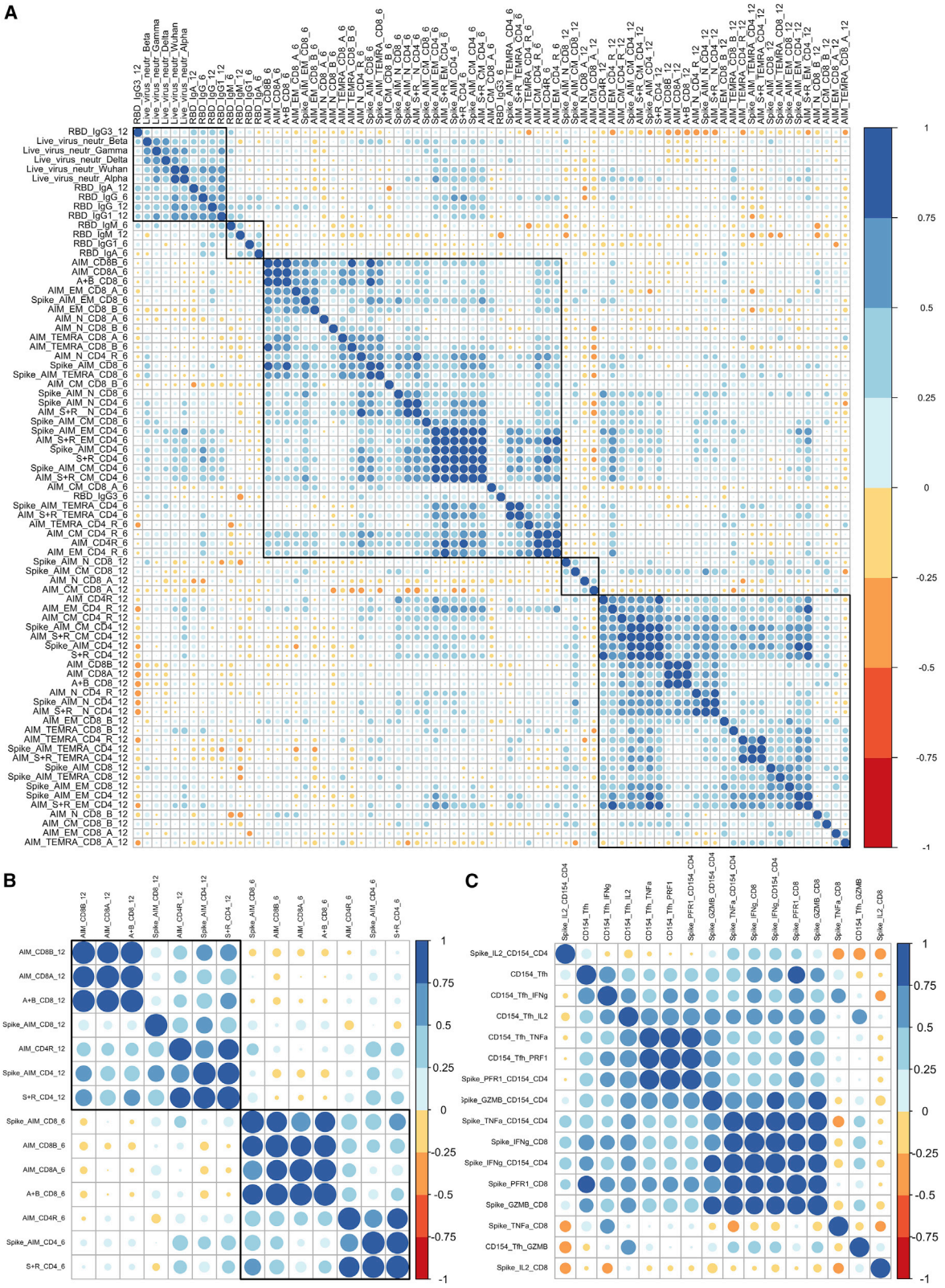

(legend on next page)

convalescents long after COVID-19 disease and, importantly, in the absence of re-infection.

Conversely, vaccination programs allow for more controlled studies and deeper immune analysis and facilitate conducting experimental procedures to test immune fitness against VOCs. However, to date, the majority of vaccinees have received spike-based vaccines, which are not well suited as a proxy for what SARS-CoV-2 immunity may look like in the long term or its adaptability to VOCs. Here, we have taken advantage of the relatively unique situation in South Australia, where local transmission of SARS-CoV-2 was eliminated early on in the pandemic in 2020, enabling us to conduct a 12 month longitudinal study of SARS-CoV-2 immunity in mild-COVID-19 convalescents and test their immune fitness against the current VOCs.

Total RBD IgG titers and other circulating Ig isotypes against SARS-CoV-2 spike and RBD antigens decrease over the months following COVID-19 disease, with the strongest decline in the first 1–3 months.[22,32,43] A concordant trend was also observed in our cohort between 6 and 12 months. A study conducted in Wuhan (China), where RBD-specific IgG was longitudinally assessed in convalescents up to 12 months post-COVID-19 in a community with absence of SARS-CoV-2 local transmission, analogous to that of South Australia, showed a similar trend between 6 and 12 months.[9] It is worth noting that the genome sequence of the virus variants causing COVID-19 in each of the studies are closely related and in the absence of VOCs. Despite declining circulating antibody titers, the majority of convalescents in our cohort (>90%) had significantly higher levels of spike- and RBD-specific total IgG compared with the healthy controls at 12 months post-COVID-19. Concomitantly, circulating RBD-specific memory B cells were present in 88.9% of convalescents, indicating that antibody responses could extend further into the future.

The presence of specific antibodies alone does not necessarily predict protection against disease. Mathematical modeling of clinical data indicates that a minimum specific Ig titer is needed for protection against COVID-19 disease.[44] This is also supported by clear evidence showing that serum virus neutralization activity, exerted by a portion of, but not all, antibodies, is the best predictor of protection.[33,42,44,45] Both live-virus and pseudovirus serum neutralization assays indicated that sera from 51% and 65%, respectively, of COVID-19 convalescents can efficiently neutralize SARS-CoV-2 bearing the spike protein homologous to one that caused the original infection at 12 months post-infection. At 6–8 months post-COVID-19, the percentage of convalescents who retain serum neutralizing activity, estimated with methods similar or identical to ours, varies considerably from ~60% to >90%.[8,22,32,46] It is important to note that these studies included more heterogeneous cohorts, which included severe COVID-19 patients. Overall, virus neutralization measures in our cohort (51%–65%) 12 months post-infection are in line with previous findings.

Recent modeling data predicted the risk of re-infection in COVID-19 convalescents to emerging variants of SARS-CoV-2 and showed that the re-infection likelihood is high, at a median time of 16 months after primary infection, earlier than for other human coronaviruses.[47] Empirical data are needed to confirm these predictions to better manage the ongoing pandemic. Although there is not unequivocal data on the risk of SARS-CoV-2 re-infection in convalescents due to the complexity of the studies in the context of this pandemic, the risk of re-infection with Omicron is significantly higher than with other VOCs that appeared earlier in the pandemic.[48]

We demonstrated with live-virus neutralization data that despite the maintenance of serum antibodies at 12 months post-infection in 90% of mild-COVID-19 convalescents, they have significantly decreased ability to neutralize the five VOCs. It is striking to see that serum neutralizing activity against B.1.1.529 is not detectable and for B.1.351 is practically non-existent. For both P.1 and B.1.617.2, the drop in the number of patients who retain serum neutralization activity is >65%. For B.1.1.7, the first VOC (chronologically), and perhaps less relevant at the present time, the reduction in neutralization titers was less pronounced. The relative differences at 12 months post-infection between the VOCs correlated well with other COVID-19 convalescent and vaccination studies.[13,14,16,18,44,49–53] Our measurements at 12 months post-COVID-19 and in the absence of re-infection reveal that although circulating SARS-CoV-2 antibody responses persist up to 12 months, the antigenic drift of SARS-CoV-2 in VOCs can efficiently bypass humoral immune responses in mild-COVID-19 convalescents.

As such, our findings stress the necessity to reinforce the immune system to overcome these insufficiencies in COVID-19 convalescents via vaccination.

Importantly, we report that SARS-CoV-2-specific circulating $CD4^+$ and $CD8^+$ T cell frequencies are maintained in a significant proportion of convalescents between 6 and 12 months post-COVID-19 and at levels reported for earlier time points,[22,23] indicating that these T cell populations are stable. While >50% of SARS-CoV-2-specific $CD4^+$ and $CD8^+$ T cells were directed at the spike protein, a significant proportion of T helper and cytotoxic T cells were activated by non-spike antigen epitopes.

Collectively, memory-compartment analysis of circulating SARS-CoV-2-specific T cells strongly suggests that in mild-COVID-19 convalescents, $CD4^+$ T_{EM}s and $CD8^+$ T_{EMRA}s have significant roles in maintaining immunity as far as 12 months after infection. Interestingly, the maintenance and large proportion of $CD8^+$ T_{EMRA}s bears resemblance to the kinetics of equivalent cells in long-term chronic infections by human CMV.[54] A significant decay of spike-specific $CD4^+$ T_{CM}s was observed; however, this was not reflected in their $CD8^+$ T cell counterparts, perhaps indicating that in the long term, cytotoxic immune function could be sustained more efficiently thanks to cell

Figure 7. Multiple immune-correlate analysis

(A) Correlations among metrics available for the full cohort (n- = 43) were analyzed and plotted as described in the STAR methods. Metrics excluded in the matrix chart were sex, age (for lack of correlation), and Omicron neutralization (all values = 0).

(B) Correlation matrix of T cell frequency data from AIM data from Figure 2.

(C) Correlation matrix of high-responder, T cell, and ICS data from Figure 5.

self-renewal and proliferation.[37] Importantly, in our cohort of high responders, T cells showed a strong capacity to produce a range of cytokines, with strong IFNγ and TNF-α responses in $CD4^+$ T cells and GZMB and PRF1 in $CD8^+$ T cells, in concordance with their respective helper and cytotoxic function profiles.

At 12 months post-infection, we did not detect significant frequencies of circulating spike-specific cT_{FH}s, even in high-responder convalescents, which is in agreement with studies that showed their decline in earlier months after infection[22] and vaccination.[55]

The current understanding of SARS-CoV-2-infection-induced T cell responses with respect to their ability to adapt to VOCs with spike antigen mutations is that contrary to antibody responses, T cells significantly maintain reactivity to such mutated antigens.[25,26] In contrast, we show, with a functional cytokine T cell assay, that changes in the spike amino-acid sequence corresponding to the VOC led to functional vulnerabilities, where even high-responder COVID-19 convalescents (4 of 15) accumulated almost half of all of these functional deficiencies. Overall, the spike-specific $CD4^+$ T cell compartment was more sensitive to VOC mutations than cytotoxic $CD8^+$ T cells. The ability to express cytokines IFNγ, TNF-α, and GZMB by $CD4^+$ T cells in response to B.1.1.529 and B.1.351 epitopes was reduced significantly. Alterations in $CD4^+$ T cell function contrasted with the lack of changes in the response mediated by GZMB or PRF1 by $CD8^+$ T cells. Perhaps, this difference is partially explained by the higher stability of $CD8^+$ T_{EM}s over time compared with their $CD4^+$ T cell counterparts.

The ability of viruses to escape virus-specific T cell responses is known.[56,57] In fact, viruses such as influenza can escape T cell responses after acquiring single amino-acid mutations.[58] Hepatitis C virus is also capable of escaping T cell responses with minimal variations to antigen amino-acid sequences.[59] Recently, in a yet-to-be-peer-reviewed study in Singapore, B.1.1529 was shown to evade SARS-CoV-2-specific cellular cytokine responses by as much as 5-fold compared with B.1617.2.[39] Our findings are concerning because additional mutations leading to the appearance of new SARS-CoV-2 variants in the future could potentially increase the ability of the virus to escape pre-existing spike-specific T cell responses.

Our results regarding T cell adaptability to VOCs are limited in that we have only tested cytokine responses to a single antigen, the spike. Our AIM assay results clearly show that spike is the main driver of immune responses in convalescents, but immunity to other non-spike proteins is also important. Variation in direct T cell effector function (cytokine production) to corresponding non-spike antigenic VOC sequences was not tested, and, therefore, the combined SARS-CoV-2 protein effect of VOC mutations on T cell immune function is yet to be fully elucidated. Prior to this study, Tarke et al. conducted multiantigenic studies (including, spike, N, M, and a range of open reading frames [ORFs]) to test T cell responses to VOCs (not including B.1.617.2 or B.1.1.529), concluding that T cell reactivity to ancestral Wuhan antigen epitopes and virus variants was not significantly different. In their experimental design, they used an AIM-assay-based approach with large peptide pools, which included mutated and non-mutated epitopes. While this approach bears more resemblance to what might happen during a SARS-CoV-2 infection, it potentially masks subtle differences in T cell reactivity and the identification of individuals whose T cell responses are more severely affected by antigenic changes in the Spike antigen of VOCs.[25] Also, while the AIM assay is a powerful method to detect and quatify T cell antigen specificity, it does not measure function directly compared with ICS.

On the other hand, while testing spike alone may be a limitation when assessing convalescent responses, our results have important implications in assessing immunity elicited by most of the current vaccines administered in developed countries, which are based exclusively on the Wuhan spike protein (e.g., vaccines produced by AstraZeneca, Pfizer-BioNTech, Janssen, or Moderna). If the deficiencies reported here have an equivalent in uninfected vaccinees, then functional T cell responses could be compromised in these individuals. Future studies must address this question.

In summary, our findings reveal that despite the durability and maintenance of serum antibodies, circulating memory B cells, and T cell responses at 12 months after original infection, COVID-19 convalescents have pronounced deficiencies in functional spike-specific T cell responses and the ability to neutralize the current VOCs. As such, mild-COVID-19 convalescents are vulnerable to infection with circulating and newly emerging SARS-CoV-2 variants 12 months after recovery. The results obtained from our functional evaluation of post-COVID-19 immunity are in line with current large observational studies, which demonstrate the added protective effect of COVID-19 vaccines in previously infected individuals.[60,61] Thus, our study highlights the importance and necessity to vaccinate COVID-19 convalescents against subsequent SARS-CoV-2 infections.

Finally, it is important to consider our findings in the context of the existing worldwide inequalities in vaccine distribution, which have kept many developing countries from Africa, South East and South Central Asia, and Central America at vaccination rates <20% so far.[62] These regions are, therefore, more vulnerable to outbreaks of emerging SARS-CoV-2 variants with the ability to evade pre-existing immune responses in unvaccinated convalescents.[63,64]

Limitations of the study

The main limitation of this study is the lack of bona fide immune correlates with which to assess the impact of the loss of T cell functionality (cytokine production) on the outcome of re-infection with heterologous SARS-CoV-2 variants. Future studies using appropriate animal models may shed light in addressing this important question. Additionally, our cytokine T cell assays were restricted to the spike antigen. Despite spike being the immunodominant SARS-CoV-2 antigen, investigations should be expanded to other SARS-CoV-2 structural and non-structural proteins to reach more definite conclusions on protection afforded by post-infection immunity against antigenically different VOCs.

At this point, our study does not explain the underlying biological processes that lead to the observed biased frequency distributions of circulating memory $CD4^+$ T_{EM} and $CD8^+$ T_{EMRA} SARS-CoV-2 T cell phenotypes in mild-COVID-19 convalescents. This question is likely to be important in understanding why and how cytokine responses vary with antigenic changes.

Our analysis was restricted to mild-COVID-19 convalescents. There are significant differences in the kinetics of humoral and cell-mediated responses in other COVID-19 patients (e.g., severe or asymptomatic), and some of the conclusions of this study may not apply to these cohorts.

STAR★METHODS

Detailed methods are provided in the online version of this paper and include the following:

- KEY RESOURCE TABLE
- RESOURCE AVAILABILITY
  - Lead contact
  - Material availability
  - Data and code availability
- EXPERIMENTAL MODEL AND SUBJECT DETAILS
- METHOD DETAILS
  - SARS-CoV-2 RBD and spike protein production
  - SARS-CoV-2 RBD ELISA
  - Detection of spike- and RBD-specific memory B cells
  - SARS-CoV-2 pseudovirus neutralization assay
  - SARS-CoV-2 live-virus neutralization assay
  - SARS-CoV-2 and CMV peptide megapools
  - Activation-induced cell marker (AIM) T cell assay
  - Variant of concern spike-specific peptide pools
  - Spike-specific T follicular helper cell quantification and intracellular cytokine staining in spike high responder convalescents
- QUANTIFICATION AND STATISTICAL ANALYSIS

SUPPLEMENTAL INFORMATION

Supplemental can be found online at https://doi.org/10.1016/j.xcrm.2022.100651.

ACKNOWLEDGMENTS

This work was funded by project grants from The Hospital Research Foundation and Women's and Children's Hospital Foundation, Adelaide, Australia. M.G.M. is a THRF Early Career Fellow. B.G.-B. is a THRF Mid-Career Fellow. We would like to thank Ms. Suzanne Edwards, University of Adelaide, for statistical advice and analysis. This project has been supported partly with federal funds from the National Institute of Allergy and Infectious Diseases, National Institutes of Health, Department of Health and Human Services, under contract nos. 75N93021C00016 to A.S. and 75N9301900065 to A.S. and D.W.

AUTHOR CONTRIBUTIONS

Writing original manuscript draft, P.G.-V., B.G.-B., and M.G.M.; editing manuscript, S.C.B., C.M.H., M.R.B., C.K.-L., E.J.G., G.M., and D.J.L.; design of experiments, P.G.-V., C.M.H., M.G.M., A.S., D.W., S.G.T., B.G.-B., S.C.B., and R.A.B.; performed experiments, P.G.-V., C.M.H., M.G.M., A.E.L.Y., H.B., Z.A.M., Z.A.-D., A. Abayasingam, A.O.S., A. Aggarwal, and D.A.; data analysis, P.G.-V., C.M.H., A.E.L.Y., G.B., B.G.-B., and R.A.B.; patient sample collection, C.M.H., J.G., C.F., S.O., E.M.M., B.A.J.R., D.S., and C.K.-L. All authors reviewed, discussed, and agreed with the manuscript.

DECLARATION OF INTERESTS

A.S. is currently a consultant for Gritstone, Flow Pharma, Arcturus, Epitogenesis, Oxfordimmunotech, Caprion, and Avalia. La Jolla Institute for Immunology (A.S. and D.W.) has filed for patent protection for various aspects of T cell epitope and vaccine design work. P.G.-V., C.M.H., M.G.M., A.E.L.Y., H.B., Z.A.M., Z.A.-D., A. Abayasingam, D.A., A.O.S., A. Aggarwal, G.B., J.G., C.F., S.O., E.M.M., D.J.L., G.M., E.J.G., B.A.J.R., D.S., C.K.-L., S.G.T., M.R.B., D.W., R.A.B., S.C.B., and B.G.-B. declare no conflicts of interest.

INCLUSION AND DIVERSITY

Inclusion of investigators and the assignment of their roles and authorship in this study was done based on their qualifications and research experience and without discriminating based on ethnic, gender, sexual orientation, or religious belief as mandated by Australian law and in conformity with the Australian Code for the Responsible Conduct of Research and the core ethical principles of the institutions involved.

Received: December 8, 2021
Revised: March 24, 2022
Accepted: May 11, 2022
Published: May 17, 2022

REFERENCES

1. Zhou, P., Yang, X.L., Wang, X.G., Hu, B., Zhang, L., Zhang, W., Si, H.R., Zhu, Y., Li, B., Huang, C.L., et al. (2020). A pneumonia outbreak associated with a new coronavirus of probable bat origin. Nature *579*, 270–273. https://doi.org/10.1038/s41586-020-2012-7.
2. Huang, X., Shao, X., Xing, L., Hu, Y., Sin, D.D., and Zhang, X. (2021). The impact of lockdown timing on COVID-19 transmission across US counties. EClinicalMedicine *38*, 101035. https://doi.org/10.1016/j.eclinm.2021.101035.
3. Rossman, H., Shilo, S., Meir, T., Gorfine, M., Shalit, U., and Segal, E. (2021). COVID-19 dynamics after a national immunization program in Israel. Nat. Med. *27*, 1055–1061. https://doi.org/10.1038/s41591-021-01337-2.
4. Barandalla, I., Alvarez, C., Barreiro, P., de Mendoza, C., González-Crespo, R., and Soriano, V. (2021). Impact of scaling up SARS-CoV-2 vaccination on COVID-19 hospitalizations in Spain. Int. J. Infect. Dis. *112*, 81–88. https://doi.org/10.1016/j.ijid.2021.09.022.
5. Pritchard, E., Matthews, P.C., Stoesser, N., Eyre, D.W., Gethings, O., Vihta, K.-D., Jones, J., House, T., VanSteenHouse, H., Bell, I., et al. (2021). Impact of vaccination on new SARS-CoV-2 infections in the United Kingdom. Nat. Med. *27*, 1370–1378. https://doi.org/10.1038/s41591-021-01410-w.
6. Bahl, A., Johnson, S., Maine, G., Garcia, M.H., Nimmagadda, S., Qu, L., and Chen, N.W. (2021). Vaccination reduces need for emergency care in breakthrough COVID-19 infections: a multicenter cohort study. Lancet Reg. Health. Am. *4*, 100065. https://doi.org/10.1016/j.lana.2021.100065.
7. Doroshenko, A. (2021). The combined effect of vaccination and nonpharmaceutical public health interventions—ending the COVID-19 pandemic. JAMA Netw. Open *4*, e2111675. https://doi.org/10.1001/jamanetworkopen.2021.11675.
8. Lau, E.H.Y., Tsang, O.T.Y., Hui, D.S.C., Kwan, M.Y.W., Chan, W.-h., Chiu, S.S., Ko, R.L.W., Chan, K.H., Cheng, S.M.S., Perera, R.A.P.M., et al. (2021). Neutralizing antibody titres in SARS-CoV-2 infections. Nat. Commun. *12*, 63. https://doi.org/10.1038/s41467-020-20247-4.
9. Li, C., Yu, D., Wu, X., Liang, H., Zhou, Z., Xie, Y., Li, T., Wu, J., Lu, F., Feng, L., et al. (2021). Twelve-month specific IgG response to SARS-CoV-2 receptor-binding domain among COVID-19 convalescent plasma donors in Wuhan. Nat. Commun. *12*, 4144. https://doi.org/10.1038/s41467-021-24230-5.
10. Naaber, P., Tserel, L., Kangro, K., Sepp, E., Jurjenson, V., Adamson, A., Haljasmagi, L., Rumm, A.P., Maruste, R., Karner, J., et al. (2021). Dynamics of antibody response to BNT162b2 vaccine after six months: a longitudinal prospective study. Lancet Reg. Health Eur. *10*, 100208. https://doi.org/10.1016/j.lanepe.2021.100208.

11. Israel, A., Shenhar, Y., Green, I., Merzon, E., Golan-Cohen, A., Schäffer, A.A., Ruppin, E., Vinker, S., and Magen, E. (2021). Large-scale study of antibody titer decay following BNT162b2 mRNA vaccine or SARS-CoV-2 infection. Preprint at medRxiv. 2021.2008. https://doi.org/10.1101/2021.08.19.21262111.

12. Liu, Y., Liu, J., Xia, H., Zhang, X., Fontes-Garfias, C.R., Swanson, K.A., Cai, H., Sarkar, R., Chen, W., Cutler, M., et al. (2021). Neutralizing activity of BNT162b2-elicited serum. N. Engl. J. Med. *384*, 1466–1468. https://doi.org/10.1056/NEJMc2102017.

13. Hammerschmidt, S.I., Bosnjak, B., Bernhardt, G., Friedrichsen, M., Ravens, I., Dopfer-Jablonka, A., Hoffmann, M., Pöhlmann, S., Behrens, G.M.N., and Förster, R. (2021). Neutralization of the SARS-CoV-2 Delta variant after heterologous and homologous BNT162b2 or ChAdOx1 nCoV-19 vaccination. Cell. Mol. Immunol. *18*, 2455–2456. https://doi.org/10.1038/s41423-021-00755-z.

14. Planas, D., Veyer, D., Baidaliuk, A., Staropoli, I., Guivel-Benhassine, F., Rajah, M.M., Planchais, C., Porrot, F., Robillard, N., Puech, J., et al. (2021). Reduced sensitivity of SARS-CoV-2 variant Delta to antibody neutralization. Nature *596*, 276–280. https://doi.org/10.1038/s41586-021-03777-9.

15. Davis, C., Logan, N., Tyson, G., Orton, R., Harvey, W., Haughney, J., Perkins, J., The, C.-G.U.K.C., Peacock, T.P., Barclay, W.S., et al. (2021). Reduced neutralisation of the Delta (B.1.617.2) SARS-CoV-2 variant of concern following vaccination. Preprint at medRxiv. https://doi.org/10.1101/2021.06.23.21259327.

16. Shen, X., Tang, H., Pajon, R., Smith, G., Glenn, G.M., Shi, W., Korber, B., and Montefiori, D.C. (2021). Neutralization of SARS-CoV-2 variants B.1.429 and B.1.351. N. Engl. J. Med. *384*, 2352–2354. https://doi.org/10.1056/NEJMc2103740.

17. Yadav, P.D., Sapkal, G.N., Ella, R., Sahay, R.R., Nyayanit, D.A., Patil, D.Y., Deshpande, G., Shete, A.M., Gupta, N., Mohan, V.K., et al. (2021). Neutralization of Beta and Delta variant with sera of COVID-19 recovered cases and vaccinees of inactivated COVID-19 vaccine BBV152/Covaxin. J. Trav. Med. *28*, taab104. https://doi.org/10.1093/jtm/taab104.

18. Bates, T.A., Leier, H.C., Lyski, Z.L., McBride, S.K., Coulter, F.J., Weinstein, J.B., Goodman, J.R., Lu, Z., Siegel, S.A.R., Sullivan, P., et al. (2021). Neutralization of SARS-CoV-2 variants by convalescent and BNT162b2 vaccinated serum. Nat. Commun. *12*, 5135. https://doi.org/10.1038/s41467-021-25479-6.

19. Shinde, V., Bhikha, S., Hoosain, Z., Archary, M., Bhorat, Q., Fairlie, L., Lalloo, U., Masilela, M.S.L., Moodley, D., Hanley, S., et al. (2021). Efficacy of NVX-CoV2373 Covid-19 vaccine against the B.1.351 variant. N. Engl. J. Med. *384*, 1899–1909. https://doi.org/10.1056/NEJMoa2103055.

20. Tarke, A., Sidney, J., Kidd, C.K., Dan, J.M., Ramirez, S.I., Yu, E.D., Mateus, J., da Silva Antunes, R., Moore, E., Rubiro, P., et al. (2021). Comprehensive analysis of T cell immunodominance and immunoprevalence of SARS-CoV-2 epitopes in COVID-19 cases. Cell Rep. Med. *2*, 100204. https://doi.org/10.1016/j.xcrm.2021.100204.

21. Grifoni, A., Sidney, J., Zhang, Y., Scheuermann, R.H., Peters, B., and Sette, A. (2020). A sequence homology and bioinformatic approach can predict candidate targets for immune responses to SARS-CoV-2. Cell Host Microbe *27*, 671–680.e2. https://doi.org/10.1016/j.chom.2020.03.002.

22. Dan, J.M., Mateus, J., Kato, Y., Hastie, K.M., Yu, E.D., Faliti, C.E., Grifoni, A., Ramirez, S.I., Haupt, S., Frazier, A., et al. (2021). Immunological memory to SARS-CoV-2 assessed for up to 8 months after infection. Science *371*, eabf4063. https://doi.org/10.1126/science.abf4063.

23. Grifoni, A., Weiskopf, D., Ramirez, S.I., Mateus, J., Dan, J.M., Moderbacher, C.R., Rawlings, S.A., Sutherland, A., Premkumar, L., Jadi, R.S., et al. (2020). Targets of T Cell responses to SARS-CoV-2 coronavirus in humans with COVID-19 disease and unexposed individuals. Cell *181*, 1489–1501.e15. https://doi.org/10.1016/j.cell.2020.05.015.

24. Grifoni, A., Sidney, J., Vita, R., Peters, B., Crotty, S., Weiskopf, D., and Sette, A. (2021). SARS-CoV-2 human T cell epitopes: adaptive immune response against COVID-19. Cell Host Microbe *29*, 1076–1092. https://doi.org/10.1016/j.chom.2021.05.010.

25. Tarke, A., Sidney, J., Methot, N., Yu, E.D., Zhang, Y., Dan, J.M., Goodwin, B., Rubiro, P., Sutherland, A., Wang, E., et al. (2021). Impact of SARS-CoV-2 variants on the total CD4+ and CD8+ T cell reactivity in infected or vaccinated individuals. Cell Rep. Med. *2*, 100355. https://doi.org/10.1016/j.xcrm.2021.100355.

26. Geers, D., Shamier, M.C., Bogers, S., den Hartog, G., Gommers, L., Nieuwkoop, N.N., Schmitz, K.S., Rijsbergen, L.C., van Osch, J.A.T., Dijkhuizen, E., et al. (2021). SARS-CoV-2 variants of concern partially escape humoral but not T cell responses in COVID-19 convalescent donors and vaccine recipients. Sci. Immunol. *6*, eabj1750. https://doi.org/10.1126/sciimmunol.abj1750.

27. Le Bert, N., Tan, A.T., Kunasegaran, K., Tham, C.Y.L., Hafezi, M., Chia, A., Chng, M.H.Y., Lin, M., Tan, N., Linster, M., et al. (2020). SARS-CoV-2-specific T cell immunity in cases of COVID-19 and SARS, and uninfected controls. Nature *584*, 457–462. https://doi.org/10.1038/s41586-020-2550-z.

28. Bar-On, Y.M., Goldberg, Y., Mandel, M., Bodenheimer, O., Freedman, L., Kalkstein, N., Mizrahi, B., Alroy-Preis, S., Ash, N., Milo, R., and Huppert, A. (2021). Protection of BNT162b2 vaccine booster against Covid-19 in Israel. N. Engl. J. Med. *385*, 1393–1400. https://doi.org/10.1056/NEJMoa2114255.

29. van Riel, D., and de Wit, E. (2020). Next-generation vaccine platforms for COVID-19. Nat. Mater. *19*, 810–812. https://doi.org/10.1038/s41563-020-0746-0.

30. Heinz, F.X., and Stiasny, K. (2021). Distinguishing features of current COVID-19 vaccines: knowns and unknowns of antigen presentation and modes of action. NPJ Vaccines *6*, 104. https://doi.org/10.1038/s41541-021-00369-6.

31. Australia, G.o.S. (2021). https://www.covid-19.sa.gov.au/home/dashboard.

32. Abayasingam, A., Balachandran, H., Agapiou, D., Hammoud, M., Rodrigo, C., Keoshkerian, E., Li, H., Brasher, N.A., Christ, D., Rouet, R., et al. (2021). Long-term persistence of RBD+ memory B cells encoding neutralizing antibodies in SARS-CoV-2 infection. Medicine *2*, 100228. https://doi.org/10.1016/j.xcrm.2021.100228.

33. Sette, A., and Crotty, S. (2021). Adaptive immunity to SARS-CoV-2 and COVID-19. Cell *184*, 861–880. https://doi.org/10.1016/j.cell.2021.01.007.

34. Saini, S.K., Hersby, D.S., Tamhane, T., Povlsen, H.R., Hernandez, S.P.A., Nielsen, M., Gang, A.O., and Hadrup, S.R. (2021). SARS-CoV-2 genome-wide T cell epitope mapping reveals immunodominance and substantial CD8(+) T cell activation in COVID-19 patients. Sci. Immunol. *6*, eabf7550. https://doi.org/10.1126/sciimmunol.abf7550.

35. Carrasco Pro, S., Sidney, J., Paul, S., Lindestam Arlehamn, C., Weiskopf, D., Peters, B., and Sette, A. (2015). Automatic generation of validated specific epitope sets. J. Immunol. Res. *2015*, 763461. https://doi.org/10.1155/2015/763461.

36. Jung, J.H., Rha, M.-S., Sa, M., Choi, H.K., Jeon, J.H., Seok, H., Park, D.W., Park, S.-H., Jeong, H.W., Choi, W.S., and Shin, E.-C. (2021). SARS-CoV-2-specific T cell memory is sustained in COVID-19 convalescent patients for 10 months with successful development of stem cell-like memory T cells. Nat. Commun. *12*, 4043. https://doi.org/10.1038/s41467-021-24377-1.

37. Kumar, B.V., Connors, T.J., and Farber, D.L. (2018). Human T cell development, localization, and function throughout life. Immunity *48*, 202–213. https://doi.org/10.1016/j.immuni.2018.01.007.

38. Juno, J.A., Tan, H.X., Lee, W.S., Reynaldi, A., Kelly, H.G., Wragg, K., Esterbauer, R., Kent, H.E., Batten, C.J., Mordant, F.L., et al. (2020). Humoral and circulating follicular helper T cell responses in recovered patients with COVID-19. Nat. Med. *26*, 1428–1434. https://doi.org/10.1038/s41591-020-0995-0.

39. Le Bert, N., Tan, A., Kunasegaran, K., Chia, A., Tan, N., Chen, Q., Hang, S.K., Qui, M.D.C., Chan, B.S.W., Low, J.G.H., et al. (2022). Mutations of

SARS-CoV-2 variants of concern escaping Spike-specific T cells. Preprint at bioRxiv. https://doi.org/10.1101/2022.01.20.477163.

40. Vitale, J., Mumoli, N., Clerici, P., De Paschale, M., Evangelista, I., Cei, M., and Mazzone, A. (2021). Assessment of SARS-CoV-2 reinfection 1 Year after primary infection in a population in Lombardy, Italy. JAMA Intern. Med. *181*, 1407. https://doi.org/10.1001/jamainternmed.2021.2959.

41. Lumley, S.F., O'Donnell, D., Stoesser, N.E., Matthews, P.C., Howarth, A., Hatch, S.B., Marsden, B.D., Cox, S., James, T., Warren, F., et al. (2021). Antibody status and incidence of SARS-CoV-2 infection in health care workers. N. Engl. J. Med. *384*, 533–540. https://doi.org/10.1056/NEJMoa2034545.

42. Hall, V.J., Foulkes, S., Charlett, A., Atti, A., Monk, E.J.M., Simmons, R., Wellington, E., Cole, M.J., Saei, A., Oguti, B., et al. (2021). SARS-CoV-2 infection rates of antibody-positive compared with antibody-negative health-care workers in England: a large, multicentre, prospective cohort study (SIREN). Lancet *397*, 1459–1469. https://doi.org/10.1016/S0140-6736(21)00675-9.

43. Wheatley, A.K., Juno, J.A., Wang, J.J., Selva, K.J., Reynaldi, A., Tan, H.X., Lee, W.S., Wragg, K.M., Kelly, H.G., Esterbauer, R., et al. (2021). Evolution of immune responses to SARS-CoV-2 in mild-moderate COVID-19. Nat. Commun. *12*, 1162. https://doi.org/10.1038/s41467-021-21444-5.

44. Khoury, D.S., Cromer, D., Reynaldi, A., Schlub, T.E., Wheatley, A.K., Juno, J.A., Subbarao, K., Kent, S.J., Triccas, J.A., and Davenport, M.P. (2021). Neutralizing antibody levels are highly predictive of immune protection from symptomatic SARS-CoV-2 infection. Nat. Med. *27*, 1205–1211. https://doi.org/10.1038/s41591-021-01377-8.

45. Deng, W., Bao, L., Liu, J., Xiao, C., Liu, J., Xue, J., Lv, Q., Qi, F., Gao, H., Yu, P., et al. (2020). Primary exposure to SARS-CoV-2 protects against reinfection in rhesus macaques. Science *369*, 818–823. https://doi.org/10.1126/science.abc5343.

46. Tea, F., Ospina Stella, A., Aggarwal, A., Ross Darley, D., Pilli, D., Vitale, D., Merheb, V., Lee, F.X.Z., Cunningham, P., Walker, G.J., et al. (2021). SARS-CoV-2 neutralizing antibodies: longevity, breadth, and evasion by emerging viral variants. PLoS Med. *18*, e1003656. https://doi.org/10.1371/journal.pmed.1003656.

47. Townsend, J.P., Hassler, H.B., Wang, Z., Miura, S., Singh, J., Kumar, S., Ruddle, N.H., Galvani, A.P., and Dornburg, A. (2021). The durability of immunity against reinfection by SARS-CoV-2: a comparative evolutionary study. Lancet. Microbe *2*, e666–e675. https://doi.org/10.1016/S2666-5247(21)00219-6(21)00219-6.

48. Altarawneh, H.N., Chemaitelly, H., Hasan, M.R., Ayoub, H.H., Qassim, S., AlMukdad, S., Coyle, P., Yassine, H.M., Al-Khatib, H.A., Benslimane, F.M., et al. (2022). Protection against the Omicron variant from previous SARS-CoV-2 infection. N. Engl. J. Med. *386*, 1288–1290. https://doi.org/10.1056/NEJMc2200133.

49. Gasser, R., Cloutier, M., Prevost, J., Fink, C., Ducas, E., Ding, S., Dussault, N., Landry, P., Tremblay, T., Laforce-Lavoie, A., et al. (2021). Major role of IgM in the neutralizing activity of convalescent plasma against SARS-CoV-2. Cell Rep. *34*, 108790. https://doi.org/10.1016/j.celrep.2021.108790.

50. Andreano, E., Piccini, G., Licastro, D., Casalino, L., Johnson, N.V., Paciello, I., Monego, S.D., Pantano, E., Manganaro, N., Manenti, A., et al. (2020). SARS-CoV-2 escape in vitro from a highly neutralizing COVID-19 convalescent plasma. Preprint at bioRxiv. 2020.2012.2028.424451. https://doi.org/10.1101/2020.12.28.424451.

51. Liu, C., Ginn, H.M., Dejnirattisai, W., Supasa, P., Wang, B., Tuekprakhon, A., Nutalai, R., Zhou, D., Mentzer, A.J., Zhao, Y., et al. (2021). Reduced neutralization of SARS-CoV-2 B.1.617 by vaccine and convalescent serum. Cell *184*, 4220–4236.e13. https://doi.org/10.1016/j.cell.2021.06.020.

52. Planas, D., Saunders, N., Maes, P., Guivel-Benhassine, F., Planchais, C., Buchrieser, J., Bolland, W.-H., Porrot, F., Staropoli, I., Lemoine, F., et al. (2022). Considerable escape of SARS-CoV-2 Omicron to antibody neutralization. Nature *602*, 671–675. https://doi.org/10.1038/s41586-021-04389-z.

53. Cele, S., Jackson, L., Khoury, D.S., Khan, K., Moyo-Gwete, T., Tegally, H., San, J.E., Cromer, D., Scheepers, C., Amoako, D.G., et al. (2022). Omicron extensively but incompletely escapes Pfizer BNT162b2 neutralization. Nature *602*, 654–656. https://doi.org/10.1038/s41586-021-04387-1.

54. Gordon, C.L., Miron, M., Thome, J.J.C., Matsuoka, N., Weiner, J., Rak, M.A., Igarashi, S., Granot, T., Lerner, H., Goodrum, F., and Farber, D.L. (2017). Tissue reservoirs of antiviral T cell immunity in persistent human CMV infection. J. Exp. Med. *214*, 651–667. https://doi.org/10.1084/jem.20160758.

55. Goel, R.R., Painter, M.M., Apostolidis, S.A., Mathew, D., Meng, W., Rosenfeld, A.M., Lundgreen, K.A., Reynaldi, A., Khoury, D.S., Pattekar, A., et al. (2021). mRNA vaccines induce durable immune memory to SARS-CoV-2 and variants of concern. Science *374*, eabm0829. https://doi.org/10.1126/science.abm0829.

56. Collins, D.R., Gaiha, G.D., and Walker, B.D. (2020). CD8+ T cells in HIV control, cure and prevention. Nat. Rev. Immunol. *20*, 471–482. https://doi.org/10.1038/s41577-020-0274-9.

57. Ciurea, A., Hunziker, L., Martinic, M.M.A., Oxenius, A., Hengartner, H., and Zinkernagel, R.M. (2001). CD4+ T-cell–epitope escape mutant virus selected in vivo. Nat. Med. *7*, 795–800. https://doi.org/10.1038/89915.

58. Price, G.E., Ou, R., Jiang, H., Huang, L., and Moskophidis, D. (2000). Viral escape by selection of cytotoxic T cell-resistant variants in influenza A virus pneumonia. J. Exp. Med. *191*, 1853–1868. https://doi.org/10.1084/jem.191.11.1853.

59. Uebelhoer, L., Han, J.H., Callendret, B., Mateu, G., Shoukry, N.H., Hanson, H.L., Rice, C.M., Walker, C.M., and Grakoui, A. (2008). Stable cytotoxic T cell escape mutation in hepatitis C virus is linked to maintenance of viral fitness. PLoS Pathog. *4*, e1000143. https://doi.org/10.1371/journal.ppat.1000143.

60. Bozio, C.H., Grannis, S.J., Naleway, A.L., Ong, T.C., Butterfield, K.A., DeSilva, M.B., Natarajan, K., Yang, D.H., Rao, S., Klein, N.P., et al. (2021). Laboratory-confirmed COVID-19 among adults hospitalized with COVID-19–like illness with infection-induced or mRNA vaccine-induced SARS-CoV-2 immunity — Nine States, January–September 2021. MMWR Morb. Mortal. Wkly. Rep. *70*, 1539–1544. https://www.cdc.gov/mmwr/volumes/70/wr/mm7044e1.htm.

61. Abu-Raddad, L.J., Chemaitelly, H., Ayoub, H.H., Yassine, H.M., Benslimane, F.M., Al Khatib, H.A., Tang, P., Hasan, M.R., Coyle, P., Al Kanaani, Z., et al. (2021). Association of prior SARS-CoV-2 infection with risk of breakthrough infection following mRNA vaccination in Qatar. JAMA *326*, 1930. https://doi.org/10.1001/jama.2021.19623.

62. World Health Organization (2020). WHO COVID-19 Dashboard (Geneva: World Health Organization). https://covid19.who.int/.

63. Uriu, K., Kimura, I., Shirakawa, K., Takaori-Kondo, A., Nakada, T.-a., Kaneda, A., Nakagawa, S., and Sato, K. (2021). Neutralization of the SARS-CoV-2 Mu variant by convalescent and vaccine serum. N. Engl. J. Med. *385*, 2397–2399. https://doi.org/10.1056/NEJMc2114706.

64. Bugembe, D.L., Phan, M.V.T., Ssewanyana, I., Semanda, P., Nansumba, H., Dhaala, B., Nabadda, S., O'Toole, Á.N., Rambaut, A., Kaleebu, P., and Cotten, M. (2021). Emergence and spread of a SARS-CoV-2 lineage A variant (A.23.1) with altered spike protein in Uganda. Nat. Microbiol. *6*, 1094–1101. https://doi.org/10.1038/s41564-021-00933-9.

65. Ryan, F.J., Hope, C.M., Masavuli, M.G., Lynn, M.A., Mekonnen, Z.A., Lip Yeow, A.E., Garcia-Valtanen, P., Al-Delfi, Z., Gummow, J., Ferguson, C., et al. (2021). Long-term perturbation of the peripheral immune system months after SARS-CoV-2 infection. Preprint at medRxiv. 2021.2007.https://doi.org/10.1101/2021.07.30.21261234.

66. Hope, C.M., Welch, J., Mohandas, A., Pederson, S., Hill, D., Gundsambuu, B., Eastaff-Leung, N., Grosse, R., Bresatz, S., Ang, G., et al. (2019). Peptidase inhibitor 16 identifies a human regulatory T-cell subset with reduced FOXP3 expression over the first year of recent onset type 1 diabetes. Eur. J. Immunol. *49*, eji.201948094-1250. https://doi.org/10.1002/eji.201948094.

67. Hsieh, C.L., Goldsmith, J.A., Schaub, J.M., DiVenere, A.M., Kuo, H.C., Javanmardi, K., Le, K.C., Wrapp, D., Lee, A.G., Liu, Y., et al. (2020). Structure-based design of prefusion-stabilized SARS-CoV-2 spikes. Science *369*, 1501–1505. https://doi.org/10.1126/science.abd0826.

68. Amanat, F., Stadlbauer, D., Strohmeier, S., Nguyen, T.H.O., Chromikova, V., McMahon, M., Jiang, K., Arunkumar, G.A., Jurczyszak, D., Polanco, J., et al. (2020). A serological assay to detect SARS-CoV-2 seroconversion in humans. Nat. Med. *26*, 1033–1036. https://doi.org/10.1038/s41591-020-0913-5.

69. Hoffmann, M., Kleine-Weber, H., and Pohlmann, S. (2020). A multibasic cleavage site in the spike protein of SARS-CoV-2 is essential for infection of human lung cells. Mol. Cell *78*, 779–784.e5. https://doi.org/10.1016/j.molcel.2020.04.022.

70. Keck, Z.Y., Li, S.H., Xia, J., von Hahn, T., Balfe, P., McKeating, J.A., Witteveldt, J., Patel, A.H., Alter, H., Rice, C.M., and Foung, S.K.H. (2009). Mutations in hepatitis C virus E2 located outside the CD81 binding sites lead to escape from broadly neutralizing antibodies but compromise virus infectivity. J. Virol. *83*, 6149–6160. https://doi.org/10.1128/JVI.00248-09.

71. Bartosch, B., Bukh, J., Meunier, J.C., Granier, C., Engle, R.E., Blackwelder, W.C., Emerson, S.U., Cosset, F.L., and Purcell, R.H. (2003). In vitro assay for neutralizing antibody to hepatitis C virus: evidence for broadly conserved neutralization epitopes. Proc. Natl. Acad. Sci. U. S. A *100*, 14199–14204. https://doi.org/10.1073/pnas.2335981100.

72. Kalemera, M.D., Cappella-Pujol, J., Chumbe, A., Underwood, A., Bull, R.A., Schinkel, J., Sliepen, K., and Grove, J. (2020). Optimised cell systems for the investigation of hepatitis C virus E1E2 glycoproteins. Preprint at bioRxiv. 2020.2006.2018.159442. https://doi.org/10.1101/2020.06.18.159442.

73. Crawford, K.H.D., Eguia, R., Dingens, A.S., Loes, A.N., Malone, K.D., Wolf, C.R., Chu, H.Y., Tortorici, M.A., Veesler, D., Murphy, M., et al. (2020). Protocol and Reagents for Pseudotyping Lentiviral Particles with SARS-CoV-2 Spike Protein for Neutralization Assays. Viruses *12*, 513. https://doi.org/10.3390/v12050513.

74. Hoaglin, D.C. (1993). Revising a display of multidimensional laboratory measurements to improve accuracy of perception. Methods Inf. Med. *32*, 418–420. https://doi.org/10.1055/s-0038-1634957.

75. Le, N.P.K., Herz, C., Gomes, J.V.D., Forster, N., Antoniadou, K., Mittermeier-Kleßinger, V., Mittermeier-Klessinger, V.K., Mewis, I., Dawid, C., Ulrichs, C., and Lamy, E. (2021). Comparative anti-inflammatory effects of Salix cortex extracts and acetylsalicylic acid in SARS-CoV-2 peptide and LPS-activated human in vitro systems. Int. J. Mol. Sci. *22*, 6766. https://doi.org/10.3390/ijms22136766.

76. Mateus, J., Dan, J.M., Zhang, Z., Rydyznski Moderbacher, C., Lammers, M., Goodwin, B., Sette, A., Crotty, S., and Weiskopf, D. (2021). Low-dose mRNA-1273 COVID-19 vaccine generates durable memory enhanced by cross-reactive T cells. Science *374*, eabj9853. https://doi.org/10.1126/science.abj9853.

77. Abayasingam, A., Balachandran, H., Agapiou, D., Hammoud, M., Rodrigo, C., Keoshkerian, E., Li, H., Brasher, N.A., Christ, D., Rouet, R., et al. (2021). Long-term persistence of RBD-positive memory B cells encoding neutralising antibodies in SARS-CoV-2 infection. Cell Rep. Med. *2*, 100228. https://doi.org/10.1016/j.xcrm.2021.100228.

STAR★METHODS

KEY RESOURCE TABLE

REAGENT or RESOURCE	SOURCE	IDENTIFIER
Antibodies		
CD8, RPA-T8, BUV395	BD Biosciences	Cat# 563795, RRID:AB_2722501
CD4, SK3, BUV496	BD Biosciences	Cat# 612936, RRID:AB_2870220
CD3, UCHT1, BUV737	BD Biosciences	Cat# 612750, RRID:AB_2870081
CD137/41BB, 4B4-1, BV421	BD Biosciences	Cat# 564091, RRID:AB_2722503
CD45RA, HI100, BV650	BD Biosciences	Cat# 563963, RRID:AB_2738514
CD14, M5E2, FITC	BD Biosciences	Cat# 555397, RRID:AB_395798
Zombie Fixable Viability Dye, N/A, GREEN	Biolegend	Cat# 423112
CD19, HIB19, FITC	BD Biosciences	Cat# 555412, RRID:AB_395812
CD69, FN50, PE	BD Biosciences	Cat# 555531, RRID:AB_395916
CD134/OX40, ACT35, PE-Cy7	BD Biosciences	Cat# 563663, RRID:AB_2738358
CCR7, 2-L1-A, APC	BD Biosciences	Cat# 566782
CD8, RPA-T8, BUV395	BD Biosciences	Cat# 563795, RRID:AB_2722501
CD4, SK3, BUV496	BD Biosciences	Cat# 612936, RRID:AB_2870220
CD3, UCHT1, BUV737	BD Biosciences	Cat# 612750, RRID:AB_2870081
CD185/CXCR5, RF8B2, BUV563	BD Biosciences	Cat# 741316, RRID:AB_2870835
CD154/CD40L, TRAP1	Biolegend	Cat# 157002, RRID:AB_2810425
GzmB, GB11, BV421	BD Biosciences	Cat# 563389, RRID:AB_2738175
IL-2, 5344.111, BV711	BD Biosciences	Cat# 563946, RRID:AB_2738501
Perforin, B-D48, FITC	Biolegend	Cat# 353310, RRID:AB_2571967
IFN-γ, B27, PE-Cy7	BD Biosciences	Cat# 557643, RRID:AB_396760
TNF, MAb11, APC	BD Biosciences	Cat# 554514, RRID:AB_398566
Fixable Viablity Stain, N/A, FVS780	BD Biosciences	Cat# 565388
CD20, 2H7-FB1, APC-H7	BD Biosciences	Cat# 560853, RRID:AB_10561681
CD14, MΦP9, APC-H7	BD Biosciences	Cat# 560270, RRID:AB_1645465
CD21, B-ly4, BV421	BD Biosciences	Cat# 562966, RRID:AB_2737921
IgD, FA6-2, BV510	BD Biosciences	Cat# 563034, RRID:AB_2737966
CD10, HI10A, BV605	BD Biosciences	Cat# 562978, RRID:AB_2737929
CD19, SJ25C1, BV711	BD Biosciences	Cat# 563036, RRID:AB_2737968
CD20, 2H7, APC-H7	BD Biosciences	Cat# 560734, RRID:AB_1727449
IgG, G18-145, BV786	BD Biosciences	Cat# 564230, RRID:AB_2738684
CD27, N-T271, PE-CF594	BD Biosciences	Cat# 562297, RRID:AB_11154596
CD38, HIT2, PE-Cy7	BD Biosciences	Cat# 560677, RRID:AB_1727473
HLA-DR, G46-6, BB515	BD Biosciences	Cat# 564516, RRID:AB_2732846
CD3, SK7, BB700	BD Biosciences	Cat# 566575, RRID:AB_2860004
Deposited data		
Raw data for figures	Mendeley Data	http://dx.doi.org/10.17632/mvkkvjbcsg.1
Other		
Streptavidin-PE	ThermoFisher Scientific	Cat# S21388
Streptavidin-APC	BD Biosciences	Cat# 554067
Fixable Viability Stain 700	BD Biosciences	Cat# 564997
Human Fc block	BD Biosciences	Cat# 564220
Stain brilliant buffer	BD Biosciences	Cat# 566349
Biotin Protein Ligase	Genecopeia	Cat# BI001

(*Continued on next page*)

Continued

REAGENT or RESOURCE	SOURCE	IDENTIFIER
Biotinylation Kit NHS-Linker	ThermoFisher Scientific	Cat# 20217
DPBS, powder, no calcium, no magnesium	ThermoFisher	Cat# 21600044
TWEEN® 20 (for PBST)	ThermoFisher	Cat# P9416
Nunc MaxiSorp™ flat-bottom	ThermoFisher	Cat# 442404
1-Step™ Ultra TMB-ELISA Substrate Solution	ThermoFisher	Cat# 34029
RPMI 1640	ThermoFisher	Cat# 11875093
Human Ab Serum	Sigma Aldrich	Cat# H4522
Dimethyl sulfoxide (DMSO)	Sigma Aldrich	Cat# D1435
L-Glutamine (200 mM)	ThermoFisher	Cat# 25030081
Penicillin-Streptomycin (10,000 U/mL)	ThermoFisher	Cat# 15140122
Benzonase® Nuclease, ultrapure	Sigma Aldrich	Cat# E1014
Trypan Blue Solution, 0.4%	ThermoFisher	Cat# 15250061
Phytohemagglutinin-M	Sigma Aldrich	Cat# 11082132001

RESOURCE AVAILABILITY

Lead contact

Further information and requests for resources and reagents should be directed to and will be fulfilled by the lead contact A/Prof Branka Grubor-Bauk (Branka.Grubor@adelaide.edu.au).

Material availability

This study did not generate new unique reagents.

Data and code availability

Any additional information required to reanalyze the data reported in this paper is available from the lead contact upon request.

EXPERIMENTAL MODEL AND SUBJECT DETAILS

Individuals who tested positive in a nasopharyngeal swab SARS-CoV-2 RT-qPCR test in March-April 2020 at South Australian Pathology Services (Adelaide, Australia) were asked to participate in a longitudinal study to assess SARS-CoV-2-specific humoral and immune cell immune correlates (Figure 1A). In this study, whole blood specimens from 43 participants (19 male, 24 female) of (95% CI, 44.8-55.4) years of age (Figure S1) who presented mild COVID-19 symptoms according to NIH guidelines (https://www.covid19treatmentguidelines.nih.gov/overview/clinical-spectrum/) were sampled and processed at two time points 6 months apart after PCR positive test. All samples were coded and de-identified for analysis. None of the participants in this study tested positive for COVID-19 after their initial positive test. Age- and gender-matched seronegative (SARS-CoV-2 RBD and Spike) healthy controls (n = 15) were included to provide baseline levels of different immune correlates (Figure S1). Prior to this, a portion of our mild-COVID-19 convalescents participated in a separate study that included serological, immunophenotyping and whole blood RNAseq analysis (Ryan et al.,[65] 2022, #214).

Blood collection and processing at the Royal Adelaide Hospital, Women's and Children's Hospital, and The University of Adelaide were performed as previously described (Hope et al.,[66] 2019, #42). Blood was collected via phlebotomy in serum separator tubes (no additives) or ethylenediaminetetraacetic acid (EDTA) tubes and processed for serum, plasma and peripheral blood mononuclear cells (PBMCs) isolation.

Study protocols were approved by the Central Adelaide Clinical Human Research Ethics Committee (#13050) and the Women's and Children's Health Network Human research ethics (protocol HREC/19/WCHN/65), Adelaide, Australia. All participants provided written informed consent in accordance with the Declaration of Helsinki and procedures were carried out following the approved guidelines.

METHOD DETAILS

SARS-CoV-2 RBD and spike protein production

Prefusion SARS-CoV-2 Spike ectodomain (isolate WHU1, residues 1-1208) with HexaPro mutations (kindly provided by Dr Adam Wheatley)[67] was used in ELISA. SARS-CoV-2 Spike transmembrane domain removed and a C-terminal His-tag (residues 1-1273)

(kindly provided by Prof Florian Krammer)[68] was used for flow cytometric detection of Spike-specific B cells. SARS-CoV-2 RBD with C-terminal His-tag (residues 319-541; kindly provided by Prof Florian Krammer)[68] was used in ELISA and flow cytometry. Recombinant proteins were overexpressed in Expi293 cells (Thermo Fisher) and 72 h later purified by Ni-NTA affinity and size-exclusion chromatography.[19] Purified proteins were quantified using the Bradford protein assay (Bio-Rad) and analyzed by SDS-PAGE and Western blot before being stored at -80°C. Recombinant RBD was biotinylated using the Avitag as described by the manufacturer (Genecopeia), while the Spike protein was biotinylated using an EZ-Link™ Sulfo-NHS-Biotin kit.

SARS-CoV-2 RBD ELISA

To normalize assay variance between individual experiments, standardized positive and negative controls were used. The threshold was set from sera collected from 40 healthy individuals prior to 2019 (mean + 2SD), while the positive control was sera from COVID-19 convalescents, collected 12 weeks after positive COVID-19 PCR test. MaxiSorp 96-well plates were coated overnight at 4°C with 5 μg/mL of recombinant RBD protein and blocked with 5% w/v skim milk in 0.05% Tween-20/PBS (PBST) at room temperature. Heat inactivated patient sera were serially diluted in blocking buffer, added and incubated for 2h at room temperature, followed by four washes in 0.05% PBST. Secondary antibodies were diluted in 5% skim milk in PBST as follows: Goat anti-Human IgG (H+L) Secondary Antibody, HRP (1:30,000; Invitrogen); Mouse Anti-Human IgG1 Fc-HRP (1:5000, Southern Biotech), Mouse Anti-Human IgG3 Hinge-HRP (1:5,000; Southern Biotech); Goat anti-human IgM HRP (1:5,000; Sigma): Goat anti-human IgA HRP antibody (1:5,000; Sigma) and incubated for 1 h at room temperature, followed by four washes with PBS-T. Plates were developed with 1-Step™ Ultra TMB Substrate (ThermoFisher Scientific) and the reaction stopped with 2M sulphuric acid. Absorbance was measured at 450 nm using Synergy HTX Multi-Mode Microplate Reader. SARS-CoV-2 Spike and RBD endpoint titers were calculated and expressed as area under the curve (AUC) using the mean optical density (OD) reading of the first dilution from healthy normal human sera as the baseline cut-off for seropositivity. AUC calculations were performed using Prism GraphPad.

Detection of spike- and RBD-specific memory B cells

The staining method used for the detection of RBD and Spike memory B cells has been described previously.[32] In brief, biotinylated RBD and Spike proteins were incubated with Streptavidin-PE (SA-PE; Molecular probes; ThermoFisher Scientific) and Streptavidin-APC (SA-APC; BD Pharmingen) in a molar ratio of 4:1 and 2:1, respectively. Cryopreserved PBMCs were thawed rapidly in a 37°C water bath and washed with pre-warmed RPMI media supplemented with 2 mM L-glutamine, 50 IU/mL penicillin, 50 μg/mL streptomycin, and 10% heat-inactivated fetal calf serum (Sigma) then washed twice. A maximum of 1×10^7 cells were stained with Fixable Viability Stain 700 (FVS700) (BD Bioscience in a 1:1000 dilution), 5 μL Human Fc block (BD Bioscience) per 2×10^6 cells, 1 μg/mL each of RBD and Spike tetramers, 5 μL each of CD21 BV421, IgD BV510, CD10 BV605, CD19 BV711 and CD20 APC-H7, 8 μL of IgG BV786, 2 μL each of CD27 PE-CF594 and CD38 PE-Cy7, 2.5 μL HLA-DR BB515 and 0.5 μL CD3 BB700 (BD Bioscience). Cells were washed, resuspended in FACS wash buffer and the data acquired on BD FACSAria™ III. Data analysis was performed using FlowJo version 10.7.1 (TreeStar). To establish background B cell levels for each of antigens and phenotypes we performed the same analysis with PBMCs from 9 healthy control individuals. Background was calculated as: average value + 2SD.

SARS-CoV-2 pseudovirus neutralization assay

Pseudovirus neutralization assays were performed as previously described.[32] In brief, SARS-CoV-2 pseudo-particles were generated by co-transfecting expression plasmids containing SARS-CoV-2 Spike (kindly provided by Dr Markus Hoffmann)[69] and the MLV gag/pol and luciferase vectors (kindly provided by Prof. Francois-Loic Cosset)[70,71] in CD81KO 293T cells (kindly provided by Dr Joe Grove),[72] using mammalian Calphos transfection kit (Takara Bio). Transfected cells were then incubated at 32°C, 5% CO_2 with the culture supernatants containing SARS-CoV-2 virus pseudoparticles (SARS-2pp) and harvested 48 h post-transfection, concentrated 10-fold using 100,000 MWCO Vivaspin centrifugal concentrators (Sartorius) and stored at –80°C.

For neutralization assays, SARS-2pp were diluted 50-fold and incubated for 1h with heat-inactivated patient serum, followed by the addition of polybrene at a final concentration of 4 μg/mL (Sigma-Aldrich), prior to addition to 293T-ACE2 over-expressing cells (kindly provided by A/Prof Jesse Bloom).[73] 293T-ACE2 cells were seeded 24 h earlier at 1.5×10^4 cells per well in 96-well white flat-bottom plates (Sigma-Aldrich). Cells were spinoculated at 800 g for two hours and incubated for two hours at 37°C, prior to media change. After 72 h, cells were lysed with a lysis buffer (Promega) and Bright Glo reagent (Promega) was added at a 1:1 ratio. Luminescence (RLU) was measured using CLARIOstar microplate reader (BMG Labtech). Neutralization assays were performed in triplicate and outliers were excluded using the modified z-score method.[74] Percentage neutralization of SARS-2pp was calculated as (1 – RLU treatment/RLU no treatment) × 100 and the half-maximum inhibitory serum dilution (ID_{50}) was calculated for each sample. An ID_{50} positive neutralization cut-off of 22.61 was determined using ID_{50} values obtained from 19 unexposed healthy participants (mean + 2 SD).[32] ID_{50} for serum was calculated using a non-linear regression model (GraphPad Prism).

SARS-CoV-2 live-virus neutralization assay

HEK-ACE2/TMPRSS cells (Clone 24)[46] were seeded in 384-well plates at 5×10^3 cells/well in the presence of the live cell nuclear stain Hoechst-33342 dye (NucBlue, Invitrogen) at a concentration of 5% v/v. Two-fold dilutions of patient plasma samples were mixed with an equal volume of SARS-CoV-2 virus solution (1.25×10^4 TCID50/ml) and incubated at 37°C for 1 h before adding 40 μl, in duplicate, to the cells (final MOI = 0.05). Viral variants used included the key variants of concern; Alpha (B.1.1.7), Beta

(B.1.351), Gamma (P1), Delta (B.1.617.2) and Omicron (B.1.1.529), as well as 'wild-type' control virus (A.2.2) from clade A and presenting no aa mutations in Spike (similar to Wuhan ancestral variant). Plates were incubated for 24 h post infection and entire wells were imaged by high-content fluorescence microscopy, cell counts obtained with automated image analysis software, and the percentage of virus neutralization was calculated with the formula: %N = (D-(1-Q)) × 100/D, as previously described.[46] An average %N > 50% was defined as having neutralizing activity.

SARS-CoV-2 and CMV peptide megapools

SARS-CoV-2 and CMV peptide megapools were kindly provided by Prof Alessandro Sette (La Jolla Institute of Immunology, CA, USA).[23] For SARS-CoV-2 whole proteome, CD8-specific peptide pools, 628 peptides restricted to the 12 most common HLA-A and HLA-B alleles and partially covering the sequences of nsp1, nsp2, PLpro, nsp4, nsp6, nsp7, nucleocapsid phosphoprotein, 3CL, nsp8, nsp9, nsp10, nsp14, RdRpol, Hel, nsp15, nsp16, surface glycoprotein, ORF3a, ORF10, ORF6, ORF7a, ORF8, envelope protein, and membrane glycoprotein were predicted *in silico* as previously described.[21] Peptides were divided into two separate megapools, CD8_A and CD8_B. In Spike peptide pool, 15-mer peptides overlapping by 10 amino acids and covering the entire Spike protein sequence were used (total of 253 peptides). For the non-Spike SARS-CoV-2 CD4 megapool 221 15-mer restricted to seven common HLA-DR (Class II HLA) alleles and covering the entire SARS-CoV-2 proteome, except for the Spike protein, were predicted *in silico* as described previously.[21] The CD8 and CD4 human Cytomegalovirus (CMV) megapools used as a virus-positive control response consist of HLA-restricted 204 and 141 peptides.[35] All peptides were synthesized and resuspended in DMSO at 1 mg/ml.

Activation-induced cell marker (AIM) T cell assay

Thawed PBMCs were rested for 2 h at 37°C, 5% CO_2 in complete RPMI (cRPMI) medium (40 U/mL penicillin, 40 ug/mL streptomycin, 2 mM L-Glutamine) with 5% (v/v) heat-inactivated human AB serum. Cells were then plated at 10^6 PBMC/well in u-bottom 96-well plates and stimulated with 1 μg/mL of different SARS-CoV-2- megapools. Combined CD4 and CD8 cytomegalovirus (CMV) megapool (1 μg/mL) and PHA 10 μg/mL (Sigma Aldrich), were included as positive controls. An equimolar amount of dimethyl sulfoxide (DMSO, vehicle) was used as a negative control. PBMC were stimulated for 24 h at 37°C, 5% CO_2, washed and stained with Zombie Green Fixable Live/Dead Stain (L/D,Biolegend) for 20 min, RT, in the dark. Cells were then washed and stained with (CD3 BUV737, CD4 BUV496, CD8 BUV395, CD14 FITC, CD19 FITC, CD45RA BV650, CCR7 (CD197) APC, CD69 PE, CD134 (OX40) PE-Cy7, CD137 (41-BB) BV421) for 20 min, at room temperature in the dark. Fluorescence minus one (FMO) control for antigens: CD45RA, CCR7, CD134, CD69 and CD137 were added to PHA stimulated cells. PBMC were washed and FACS Fix (0.4%PFA, 20 g/L Glucose, Sodium Azide 0.02% in PBS) was added for 20 min at room temperature, in the dark. Fixed cells were washed, resuspended in FACS wash buffer and data was acquired on BD FACS Symphony. Data analysis was performed using FCS Express ™ (DeNovo Software, Pasadena, CA, USA). All percentages of activated cells were calculated subtracting unspecific DMSO background for each cell phenotype and individual patient.

Variant of concern spike-specific peptide pools

SARS-CoV-2 Spike PepTivator® protein pools (Miltenyi Biotec, Gladbach, GER) were utilized to test immune reactivity of COVID-19 convalescent T cells to mutated Spike epitopes present in five VOCs.[26,75] All peptide pools consisted of 15-mer peptides with 11 aa overlap covering Spike protein sequences affected by mutations in each VOC. Five VOC peptide pools corresponding to mutated Spike sequences in SARS-CoV-2 variants B.1.1.7, B.1.351, P.1, B.1.617.2 and B.1.1.529 (34, 30, 41, 32 and 83 peptides, respectively) and five corresponding control/reference pools with Wuhan aa sequences were compared in parallel along with whole Spike peptide pool as positive control (pool described above). Mutations and deletions represented in mutated pools are summarized in Table S1. For the assays, lyophilized peptides were resuspended in sterile miliQ water as per the manufacturer's instructions at 30 nM (50 μg/mL), aliquoted and stored at -80°C until used.

Spike-specific T follicular helper cell quantification and intracellular cytokine staining in spike high responder convalescents

According to AIM assay results, convalescents with Spike-specific $CD4^+$ and $CD8^+$ T cell frequencies above the mean plus 3*standard deviations in the healthy control group were identified. Double responders (meeting criterion for both $CD4^+$ and $CD8^+$ T cells) and high $CD4^+$ with available PBMC samples were selected (n = 15) for further analysis. Following methods similar to other published prior to this study,[76] PBMCs were thawed and prepared for cell culture as described for the AIM assay. Cells were pre-treated with 0.555 μg/mL of anti-CD40 blocking antibody (HB14, Miltenyi Biotec) for 15 min. Then, peptide pools were added to a final concentration of 1 μg/mL (making anti-CD40 concentration 0.5 μg/mL for the remainder of the stimulation period). After a 24 h incubation 2 μM GolgiStop™ (containing monensin, BD, 554724) and 1 μg/mL GolgiPlug™ (containing Brefeldin A, BD, 555029) were added to the cells and incubated for an additional 4 h. Cells were then co-incubated with Fixable Viability stain 780 (BD) and Fc Block (BD) for 20 min, RT, in the dark, washed with FACS buffer solution and stained with surface stain mix (CD3 BUV737, CD4 BUV496, CD8 BUV395, CXCR5 BUV563, CD14 APC-Cy7, CD20 APC-Cy7) for 20 min, RT, in the dark. Cells were washed with PBS and subsequently fixed and permeabilized with Cytofix/Cytoperm™ (BD, 51-2090KZ) for 20 min, RT, in the dark. Cells were then washed with Perm/Wash™ (BD, 51-2091KZ) and stained with ICS stain Mix (CD154 PE, IFNγ PE-Cy7, TNFα APC, PRF1 FITC, IL-2 BV711, GZMB BV421) for 20 min, RT, in the dark. Cells were then washed twice with Perm/Wash™ and once with

PBS. Finally, cells were resuspended in PBS and kept at 4°C until data was acquired on BD FACS Symphony. Data analysis was performed using FCS Express ™ (DeNovo Software, Pasadena, CA, USA).

QUANTIFICATION AND STATISTICAL ANALYSIS

The relative magnitude of intracellular cytokine expression in cells stimulated with VOC-specific mutated peptides (MUT) with respect of that in cells stimulated with equivalent peptide pools with amino acid sequences of ancestral SARS-CoV-2 (REF) were calculated as fold-change in the percentage of cytokine positive cells using the formula: Fold-change values.

All mild-COVID-19 patient samples available at the time points reported in the study from the South Australian cohort (n = 43) were used in this study and, therefore, no *pre hoc* power calculations were carried out to determine the sample size. A sufficient number of healthy controls (n = 15) were recruited to establish meaningful comparisons and assay cut-off and baseline levels consistent with current literature. Additional healthy controls (sampled prior to 2019) were used to validate serological, virus neutralization and B cell staining assays (see STAR Methods section). All statistical analyses were performed using GraphPad Prism 9.0.0 (San Diego, CA, US). No assumptions were made about the distribution of the data sets; non-parametric tests were used in all cases for comparisons. Accordingly, two-tailed Mann-Whitney's or Welch's tests were applied for pair-wise comparisons or Krustal-Wallis test for unpaired comparisons (HC vs patient data) of antibody and T cell frequency data. A non-linear regression model was used to calculate individual patient ID_{50} values from corresponding pseudovirus particles neutralization assay data.[77] A mixed-effects analysis was performed to carry out all pair-wise comparisons in memory B cell frequency data. Conservative multiple comparisons corrections were not applied in statistical analysis in order to avoid obscuring existing associations between different immune correlates.

Multiple variable (metrics) analysis was conducted using R, v 4.1.0 (R Core Team, 2021) using the corrplot (Wei and Simko, 2021) and psych (Revelle, 2021)packages. All correlation heatmaps were created using corrplot, with the order set using the 'hclust' (hierarchical clustering) option. Spearman's correlation coefficient was used to calculate all correlation coefficients, and a significance level of 5% was used to assess whether the correlation coefficients were significant different from 0. All p-values were corrected using a false discovery rate of 5%.

Since all samples that were available in South Australia were used in the study, no randomization was performed in the experiments. No experiments were blinded in this study.